AD-764 890

ELECTRICALLY SMALL LOOP ANTENNA LOADED BY A HOMOGENEOUS AND ISOTROPIC FERRITE CYLINDER-PART I

D. V. Giri

Harvard University

Prepared for:

Joint Services Electronics Program

July 1973

DISTRIBUTED BY:

NTIS

National Technical Information Service
U. S. DEPARTMENT OF COMMERCE
5285 Port Royal Road, Springfield Va. 22151

AD 764890

Office of Naval Research

Contract N60014-67-A-0366-0026 NR-371-019

ELECTRICALLY SMALL LOOP ANTENNA LOADED BY A HOMOGENEOUS AND ISOTROPIC FERRITE CYLINDER - PART I

By

D. H. Wyl

July 1973

Reproduced by
NATIONAL TECHNICAL
INFORMATION SERVICE
U S Department of Commerce
Springfield VA 22151

Technical Report No. 543

This document has been approved for public release and sale; its distribution is unlimited. Reproduction in whole or in part is permitted by the U. S. Government.

Division of Engineering and Applied Physics
Harvard University Cambridge, Massachusetts

Unclassified

Security Classification

DOCUMENT CONTROL DATA - R & D

(Security classification of title, body of abstract and indexing annotation must be entered when the overall report is classified)

1. ORIGINATING ACTIVITY (Corporate author)
Division of Engineering and Applied Physics
Harvard University
Cambridge, Massachusetts 02138

2a. REPORT SECURITY CLASSIFICATION
Unclassified

2b. GROUP

3. REPORT TITLE
ELECTRICALLY SMALL LOOP ANTENNA LOADED BY A HOMOGENEOUS AND ISOTROPIC FERRITE CYLINDER - PART I

4. DESCRIPTIVE NOTES (Type of report and inclusive dates)
Interim Technical Report

5. AUTHOR(S) (First name, middle initial, last name)
D. V. Giri

6. REPORT DATE
July, 1973

7a. TOTAL NO. OF PAGES
51

7b. NO. OF REFS
18

8a. CONTRACT OR GRANT NO.
N00014-67-A-0298-0005

b. PROJECT NO.

c.

d.

9a. ORIGINATOR'S REPORT NUMBER(S)
646

9b. OTHER REPORT NO(S) (Any other numbers that may be assigned this report)

10. DISTRIBUTION STATEMENT
This document has been approved for public release and sale; its distribution is unlimited. Reproduction in whole or in part is permitted by the U.S. Government.

11. SUPPLEMENTARY NOTES

12. SPONSORING MILITARY ACTIVITY
"Joint Services Electronics Program through (Adm. Service-Office of Naval Research, Air Force Office of Scientific Research or U.S. Army Elect. Command)"

13. ABSTRACT

A theoretical treatment has been developed for the problem of an electrically small loop antenna loaded by an infinitely long, homogeneous, isotropic but lossy ferrite rod. The loop which carries a constant current has been idealized to be a delta-function generator. An effective magnetic current (volts) is expressed explicitly in the form of an inverse Fourier integral. The contribution to the total current from the simple pole which can be associated with the surface wave is called the transmission current while the contribution from the branch cut giving rise to the radiated field is, correspondingly, the radiation current. Also, the asymptotic behavior of the current very near the delta-function source is investigated. Two values of electrical radii of the rod are considered and for one of the cases the magnetic current is plotted for a range of values of the permeability of the ferrite rod

DD FORM 1 NOV 65 1473 (PAGE 1)

S/N 0102-014-6700

Unclassified

Security Classification

Unclassified
Security Classification

14. KEY WORDS	LINK A ROLE	LINK A WT	LINK B ROLE	LINK B WT	LINK C ROLE	LINK C WT
Loop antenna						
Ferrite rod antenna						
Magnetic current						

DD FORM 1 NOV 65 1473 (BACK)
S/N 0102-014-6800

Unclassified
Security Classification

A-31409

Office of Naval Research

Contract N00014-67-A-0298-0005 NR-371-016

ELECTRICALLY SMALL LOOP ANTENNA LOADED BY A HOMOGENEOUS AND ISOTROPIC FERRITE CYLINDER - PART I

By

D. V. Giri

Technical Report No. 646

This document has been approved for public release and sale; its distribution is unlimited. Reproduction in whole or in part is permitted by the U. S. Government

July 1973

The research reported in this document was made possible through support extended the Division of Engineering and Applied Physics, Harvard University by the U. S. Army Research Office, the U. S. Air Force Office of Scientific Research and the U. S. Office of Naval Research under the Joint Services Electronics Program by Contracts N00014-67-A-0298-0006, 0005, and 0008.

Division of Engineering and Applied Physics

Harvard University · Cambridge, Massachusetts

ELECTRICALLY SMALL LOOP ANTENNA LOADED BY A HOMOGENEOUS AND ISOTROPIC FERRITE CYLINDER - PART I

By

D. V. Giri

Division of Engineering and Applied Physics

Harvard University · Cambridge, Massachusetts

ABSTRACT

A theoretical treatment has been developed for the problem of an electrically small loop antenna loaded by an infinitely long, homogeneous, isotropic but lossy ferrite rod. The loop which carries a constant current has been idealized to be a delta-function generator. An effective magnetic current (volts) is expressed explicitly in the form of an inverse Fourier integral. The contribution to the total current from the simple pole which can be associated with the surface wave is called the transmission current while the contribution from the branch cut giving rise to the radiated field is, correspondingly, the radiation current. Also, the asymptotic behavior of the current very near the delta-function source is investigated. Two values of electrical radii of the rod are considered and for one of the cases the magnetic current is plotted for a r nge of values of the permeability of the ferrite rod.

I. INTRODUCTION

This report addresses itself to the problem of ferrite-cored loop antennas. Circular loop antennas with permeable cores have been used extensively in radio receivers. More recently, the radiative properties of loop antennas with spherical ferrite cores have been studied both theoretically and experimentally by several researchers. Loop antennas with cylindrical ferrite cores have not been used as transmitting elements, possibly because of a lack of sufficient theoretical and experimental information.

By way of introduction, it is useful to consider an historical review of this class of antennas. In the early years of radio, receivers (540-1600 KHz) employed a flat coil of wire, usually mounted on a flat surface of the radio cabinet, as the receiving element. Since the coil was air-cored, its performance depended largely on the number of turns, coil area and Q. With the demand for compact sets, it became increasingly difficult to place large-area coils far enough away from the chassis and get appreciable sensitivities. Out of this need for smaller sets evolved the idea of using high permeability material for an antenna core and an early work reported on this subject is by Kihn, Harvey and O'Neill (1940). Their experiments involved a core of finely divided iron pressed with a binder which soon proved to be uneconomical because of the large mass of material needed for a small improvement. So, a large permeability material with a low loss was needed and found in ferrites.

Since their use in broadcast receivers, ferrite rod antennas have received only occasional attention. As transmitting elements, they have been studied more recently. However, most treatments [1]-[4] have been for spherical ferrite cores; an exception is the work of Islam [5] which treats a cylindrical ferrite core driven by a constant current carrying loop. The formulation in [5] consists of finding the magnetic vector potential $\vec{A} = \hat{\phi}A_\phi$ ex-

plicitly in an integral form. Some numerical results are also presented for the radiated field and radiation resistance at low frequencies of the order of 300 KHz. In contrast with the work of Islam [5], the present report is a direct boundary-value approach to find the electromagnetic fields everywhere. For this purpose an effective magnetic current has been defined and evaluated. At least in principle, the other quantities of interest can be derived from the magnetic current distribution if it is precisely known.

II. ELECTROMAGNETIC FIELDS OF A LOOP WITH FERRITE CORE

Figure 1 shows an electrically small, filamentary loop antenna of radius a, loaded by an infinitely long, homogeneous, isotropic but lossy ferrite rod of the same radius. The ferrite medium is characterized by $\mu = \mu_0(\mu_r' + i\mu_r'')$, $\varepsilon = \varepsilon_0(\varepsilon_r' + i\varepsilon_r'')$ and $k_1 = \omega\sqrt{\mu\varepsilon}$. The medium surrounding the rod and extending to infinity is free space, characterized by μ_0, ε_0 and $k_0 = \omega\sqrt{\mu_0\varepsilon_0}$. The radius of the loop is much less than the wavelength λ_f in the ferrite medium so that the loop current I_0^e is in phase at all points and essentially a constant. Thus, the only source of electromagnetic fields in this problem can be represented mathematically by $\hat{\phi} I_0^e \delta(\rho - a)\delta(z)$. Furthermore, there is azimuthal symmetry so that the field quantities do not vary with respect to the ϕ coordinate. An harmonic time dependence factor $\exp(-i\omega t)$ is implicit in all field quantities.

At this stage a discussion concerning the relevant field components is in order. Islam [5] states that due to the symmetry of the problem, only the ϕ component of the magnetic vector potential $\hat{A}$ exists and then proceeds to find E_ϕ, H_ρ and H_z through A_ϕ, setting all other field components equal to zero. In evaluating field quantities in certain antenna problems, it is convenient to use the component of vector potential that is parallel to the direction of the current in the antenna, namely, A_z in the case of the dipole

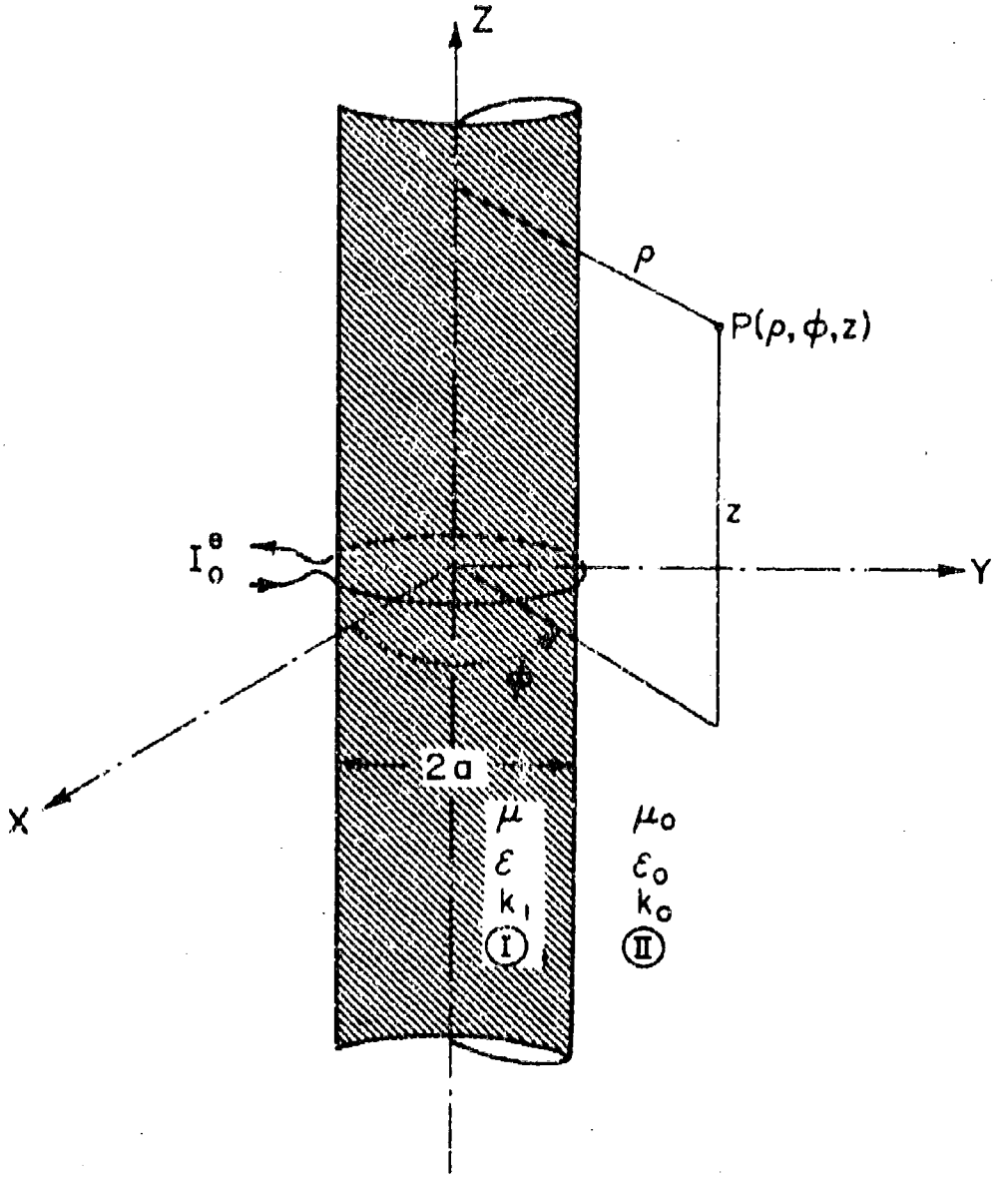

FIG. 1 GEOMETRY OF THE PROBLEM

antenna and A_ψ for a loop antenna without the core. In both these cases the parallel component is sufficient to solve the problem completely. The approach generally adopted is to set up and solve an integral equation for the current on the antenna. With the current distribution known precisely, other quantities of interest can be derived.

There are a few similarities between the conducting cylindrical dipole antenna and the ferrite-rod antenna. The dipole antenna is made up of a wire of high electrical conductivity and is driven by a delta-function voltage generator while the ferrite rod antenna consists of a material of high permeability (magnetic analog of electrical conductivity)* and is driven by a delta-function current generator. Practical metals like copper, aluminum and brass have high enough conductivities to justify an approximation of vanishing fields inside the material of the dipole antenna and, if more accuracy is required, theories do exist for imperfectly conducting dipole antennas [6], [7]. While the dipole antenna problem has been set up and solved with an integral equation, the loop loaded by a ferrite rod is a boundary-value problem formulated in terms of differential equations. However, on the basis of physical mechanisms, the ferrite-rod antenna can well be compared with the dielectric rod antenna [8]. In the ferrite material, the magnetic dipoles get aligned in the direction of the magnetic field giving rise to an effective magnetization $\vec{M}$ whereas the electric dipoles get rearranged in the dielectric medium to give rise to a polarization $\vec{P}$. This analogy will be discussed in further detail at a later stage.

Returning to the question of relevant field components, the loop carries

*Permeability can be called the magnetic analog of electrical conductivity since conductivity and permittivity can be represented interchangeably in a material or medium with complex parameters.

an azimuthal current and excites the magnetic dipoles inside the ferrite medium which can be viewed as microscopic current whirls as shown in Fig. 2. Since these currents on the antenna are in the ϕ-direction, a component of magnetic vector potential parallel to the currents, A_ϕ, is sufficient to derive all the non-vanishing field components. This is basically the reason why $E_z = 0$, $E_\rho = 0$ and $H_\phi = 0$, and H_ρ, H_z and E_ϕ must be determined by solving Maxwell's equations, appropriately written for various regions and with suitable boundary conditions. In fact, this procedure does not require a current distribution to be defined on the antenna; however, a knowledge of an equivalent current distribution on the infinite rod could perhaps be very useful in predicting the characteristics of a finite rod antenna. It is mathematically inconvenient to work with the $\nabla \times \vec{M}$ currents depicted in Fig. 2; hence, an equivalent picture given in Fig. 3 is used and the magnetic current density $\vec{M}$ is defined. It is a volumetric current with specific ρ and z dependence, which can be integrated over the cross section of the antenna to obtain an equivalent magnetic current $I_z^*(z)$ (volts). This current can be derived if the electromagnetic fields inside the ferrite rod are known. It is now necessary, therefore, to determine these fields which are solutions of Maxwell's curl equations:

$$\nabla \times \vec{E} = -\dot{\vec{B}} \tag{1}$$

$$\nabla \times \vec{H} = \vec{J} + \dot{\vec{D}} \tag{2}$$

Eliminating $\vec{H}$ from (1) and (2) gives

$$\nabla \times (\nabla \times \vec{E}) - k^2\vec{E} = i\omega\mu\vec{J} \tag{3}$$

With $\vec{J} = \hat{\phi}J_\phi = \hat{\phi}I_0^e\delta(\rho - a)\delta(z)$, $E_\rho = E_z = 0$ and $\partial/\partial\phi \equiv 0$, and using an expan-

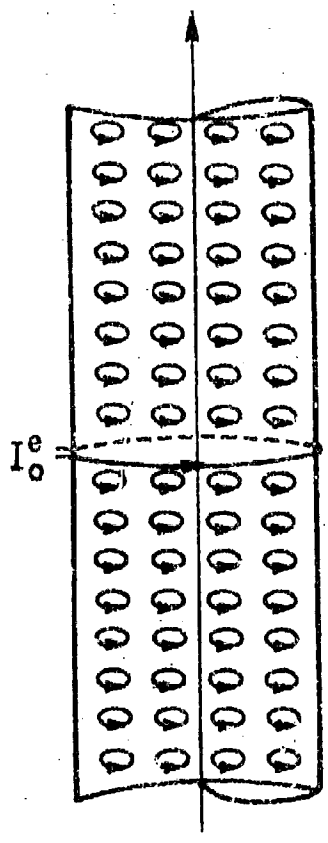

FIG. 2 MAGNETIC DIPOLES EXCITED IN THE FERRITE MEDIUM BY THE CURRENT CARRYING LOOP.

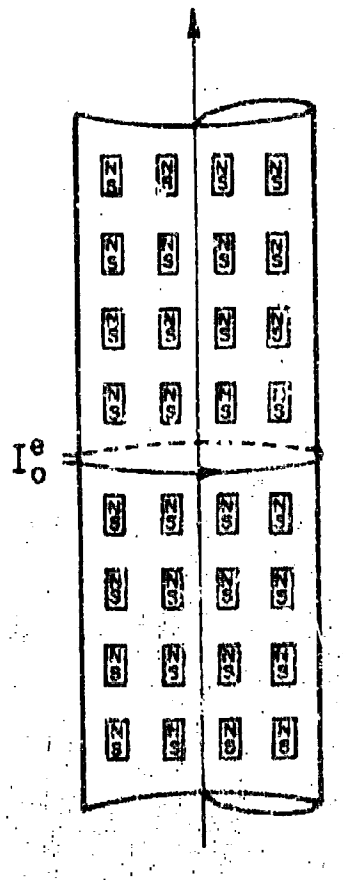

FIG. 3 AN EQUIVALENT PICTURE SHOWING NET AXIAL MAGNETIZATION.

sion in cylindrical coordinates, (3) reduces to

$$\left[\frac{\partial^2}{\partial\rho^2} + \frac{1}{\rho}\frac{\partial}{\partial\rho} + \left(k^2 - \frac{1}{\rho^2}\right) + \frac{\partial^2}{\partial z^2}\right] E_\phi(\rho,z) = -i\omega\mu J_\phi \tag{4}$$

By solving (4) for E_ϕ and using (1), H_ρ and H_z can be obtained in terms of E_ϕ as follows:

$$H_\rho = -\frac{1}{i\omega\mu}\frac{\partial E_\phi}{\partial z} \tag{5a}$$

$$H_z = \frac{1}{i\omega\mu}\left(\frac{\partial E_\phi}{\partial\rho} + \frac{E_\phi}{\rho}\right) \tag{5b}$$

In order to solve (4), a Fourier transform pair is defined as follows:

$$\bar{E}(\rho,\xi) = \int_{-\infty}^{\infty} E_\phi(\rho,z)e^{-i\xi z}\,dz \tag{6}$$

$$E_\phi(\rho,z) = \int_{-\infty}^{\infty} \frac{1}{2\pi}\,\bar{E}(\rho,\xi)e^{i\xi z}\,d\xi \tag{7}$$

The Fourier transform of (4) is

$$\left\{\frac{d^2}{d\rho^2} + \frac{1}{\rho}\frac{d}{d\rho} + \left[(k^2 - \xi^2) - \frac{1}{\rho^2}\right]\right\}\bar{E}(\rho,\xi) = -i\omega\mu I_0^e\delta(\rho - a) \tag{8}$$

Continuity of the tangential electric field requires that $\bar{E}(\rho,\xi)$ be continuous at $\rho = a$ (<u>first boundary condition</u>). The discontinuity in the tangential magnetic field is the true electric surface current density, or $H_z^{(2)} - H_z^{(1)}\Big|_{\rho=a} = -I_0^e\delta(z)$ where the superscripts refer to regions I and II as shown in Fig. 1. With (5b) this becomes

$$\frac{1}{i\omega\mu_0}\left(\frac{\partial E_\phi^{(2)}}{\partial\rho} + \frac{E_\phi^{(2)}}{\rho}\right) - \frac{1}{i\omega\mu}\left(\frac{\partial E_\phi^{(1)}}{\partial\rho} + \frac{E_\phi^{(1)}}{\rho}\right) = -I_0^e\delta(z) \tag{9}$$

The Fourier transform of (9) is

$$\left[\frac{d\bar{E}^{(2)}}{d\rho} - \frac{1}{\mu_r}\frac{d\bar{E}^{(1)}}{d\rho} + \frac{\bar{E}^{(2)}}{a} - \frac{\bar{E}^{(1)}}{a\mu_r}\right]_{\rho=a} = -i\omega\mu_0 I_0^e$$

(second boundary condition)

Now the solution for (8), which satisfies the homogeneous differential equation and is single-valued, fulfills the above boundary conditions and is well behaved at $\rho = 0$ and infinity, is

$$\bar{E}^{(1)}(\rho,\xi) = AJ_1\left(\sqrt{k_1^2 - \xi^2}\,\rho\right) \qquad \text{for } 0 \le \rho \le a \tag{10}$$

$$\bar{E}^{(2)}(\rho,\xi) = BH_1^{(1)}\left(\sqrt{k_0^2 - \xi^2}\,\rho\right) \qquad \text{for } a \le \rho \le \infty \tag{11}$$

Let $\gamma_0 = \sqrt{k_0^2 - \xi^2}$ and $\gamma_1 = \sqrt{k_1^2 - \xi^2}$. It follows from the application of the boundary conditions (see Appendix I) that

$$\begin{bmatrix} J_1(\gamma_1 a) & -H_1^{(1)}(\gamma_0 a) \\ J_1(\gamma_1 a) + a\gamma_1 J_1'(\gamma_1 a) & -[\mu_r H_1^{(1)}(\gamma_0 a) + a\mu_r\gamma_0 H_1^{(1)\prime}(\gamma_0 a)] \end{bmatrix} \begin{bmatrix} A \\ B \end{bmatrix} = \begin{bmatrix} 0 \\ i\omega\mu_0\mu_r a I_0^e \end{bmatrix}$$

This matrix equation can be solved for A and B to give

$$A = i\omega\mu a I_0^e H_1^{(1)}(\gamma_0 a)/D(\xi) \tag{12}$$

$$B = i\omega\mu a I_0^e J_1(\gamma_1 a)/D(\xi) \tag{13}$$

where $D(\xi)$ is given by

$$D(\xi) = a[\gamma_1 J_0(\gamma_1 a)H_1^{(1)}(\gamma_0 a) - \gamma_0\mu_r J_1(\gamma_1 a)H_0^{(1)}(\gamma_0 a)] \tag{14}$$

The substitution of (12) and (13) in (10) and (11) gives the transformed

fields in the two regions. Thus,

$$\bar{E}^{(1)}(\rho,\xi) = i\omega\mu a I_0^e H_1^{(1)}(\gamma_0 a) J_1(\gamma_1 \rho)/D(\xi) \tag{15}$$

$$\bar{E}^{(2)}(\rho,\xi) = i\omega\mu a I_0^e J_1(\gamma_1 a) H_1^{(1)}(\gamma_0 \rho)/D(\xi) \tag{16}$$

The application of the Fourier inversion formula gives

$$E_\phi^{(1)}(\rho,z) = \frac{i\omega\mu a I_0^e}{2\pi} \int_{-\infty}^{\infty} \frac{H_1^{(1)}(\gamma_0 a) J_1(\gamma_1 \rho)}{D(\xi)} e^{i\xi z}\, d\xi \tag{17}$$

$$E_\phi^{(2)}(\rho,z) = \frac{i\omega\mu a I_0^e}{2\pi} \int_{-\infty}^{\infty} \frac{J_1(\gamma_1 a) H_1^{(1)}(\gamma_0 \rho)}{D(\xi)} e^{i\xi z}\, d\xi \tag{18}$$

Once the preceding integrals are evaluated, the electromagnetic field is completely determined if use is made of (5a) and (5b).

III. REDUCTION OF FIELD EXPRESSION TO THE CASE OF SINGLE TURN LOOP ANTENNA IN FREE SPACE

When $\mu_r = 1$ and $\epsilon_r = 1$, the problem is equivalent to that of a loop antenna in free space. Hence, with $\mu_r = \epsilon_r = 1$ in (18) the field should reduce to that of a constant current-carrying loop antenna. In order to achieve this reduction, the quantities μ_r, ϵ_r, k_1, γ_1 and μ become 1, 1, k_0, γ_0 and μ_0, respectively. With these changes (18) becomes

$$E_\phi^{(2)}(\rho,z) = \frac{i\omega\mu_0 a I_0^e}{2\pi} \int_{-\infty}^{\infty} \frac{J_1(\gamma_0 a) H_1^{(1)}(\gamma_0 \rho) e^{i\xi z}}{\gamma_0 a [J_0(\gamma_0 a) H_1^{(1)}(\gamma_0 a) - J_1(\gamma_0 a) H_0^{(1)}(\gamma_0 a)]}\, d\xi$$

$$= -\frac{\omega\mu_0 a I_0^e}{2\pi} \int_{-\infty}^{\infty} \frac{J_1(\gamma_0 a) H_1^{(1)}(\gamma_0 \rho) e^{i\xi z}}{\gamma_0 a [J_0(\gamma_0 a) Y_0'(\gamma_0 a) - Y_0(\gamma_0 a) J_0'(\gamma_0 a)]}\, d\xi$$

where the term within the brackets in the denominator is a Wronskian and is

equal to $(2/\pi a\gamma_0)$. Therefore,

$$E_\phi^{(2)}(\rho,z) = (-\omega\mu_0 a I_0^e/4) \int_{-\infty}^{\infty} J_1(\gamma_0 a) H_1^{(1)}(\gamma_0\rho) e^{i\xi z}\, d\xi$$

For a distant point ($a \ll z,\rho$) and a thin antenna ($k_0 a \ll 1$) the small argument approximation for $J_1(\gamma_0 a) \simeq (\gamma_0 a/2)$ applies and

$$E_\phi^{(2)}(\rho,z) \simeq (-\omega\mu_0 a^2 I_0^e/8) \int_{-\infty}^{\infty} \sqrt{k_0^2 - \xi^2}\, H_1^{(1)}\left(\rho\sqrt{k_0^2 - \xi^2}\right) e^{i\xi z}\, d\xi \qquad (19)$$

The foregoing integral may be evaluated using Weyrich's formula [9],

$$\frac{1}{2}\int_{-\infty}^{\infty} e^{i\xi z} H_0^{(1)}\left(\rho\sqrt{k_0^2 - \xi^2}\right) d\xi = \frac{\exp(ik_0\sqrt{\rho^2 + z^2})}{\sqrt{\rho^2 + z^2}}$$

which is valid for ρ and z real; $0 \le \arg k_0 < \pi$; $0 \le \arg\sqrt{k_0^2 - \xi^2} < \pi$. If this formula is differentiated on both sides with respect to ρ, the result is

$$-\frac{1}{2}\int_{-\infty}^{\infty} e^{i\xi z} H_1^{(1)}\left(\rho\sqrt{k_0^2 - \xi^2}\right)\sqrt{k_0^2 - \xi^2}\, d\xi = \frac{d}{d\rho}\left[\frac{\exp(ik_0\sqrt{\rho^2 + z^2})}{\sqrt{\rho^2 + z^2}}\right]$$

$$\int_{-\infty}^{\infty} e^{i\xi z} H_1^{(1)}\left(\rho\sqrt{k_0^2 - \xi^2}\right)\sqrt{k_0^2 - \xi^2}\, d\xi = \frac{2}{i}\left[\frac{\rho}{(\rho^2 + z^2)^{3/2}} - \frac{ik_0\rho}{\rho^2 + z^2}\right] e^{ik_0\sqrt{\rho^2 + z^2}}$$

When this result is substituted in (19), one obtains

$$E_\phi^{(2)}(\rho,z) = (i\omega\mu_0 a^2 I_0^e/4)\left[\frac{\rho}{(\rho^2 + z^2)^{3/2}} - \frac{ik_0\rho}{\rho^2 + z^2}\right] \exp(ik_0\sqrt{\rho^2 + z^2})$$

This expression is in cylindrical coordinates and can easily be put in spherical coordinates by letting $\rho = R\sin\theta$ and $\rho^2 + z^2 = R^2$,

$$E_\phi^{(2)}(R,\theta) = (i\omega\mu_0 a^2 I_0^e/4)\left[\frac{R\sin\theta}{R^3} - \frac{ik_0 R\sin\theta}{R^2}\right] e^{ik_0 R}$$

$$= \left(\frac{i\omega\mu_0 I_0^e}{4\pi R^2} \pi a^2 \right) (1 - ik_0 R) \sin\theta \, e^{ik_0 R} \tag{20}$$

This is the usual form for the far field of a current loop in free space and is in agreement with the results obtained by King [10] and Wait [11].

IV. MAGNETIC CURRENT ON THE FERRITE ROD

From the knowledge of the electric field inside the ferrite rod, the magnetic current in the antenna can be found. As pointed out in Section II, a knowledge of this current could be useful in order to predict the characteristics of a finite rod antenna. The following procedure is adopted in finding the current $I_z^*(z)$: 1) since $E_\phi^{(1)}$ is known, $H_z^{(1)}$ can be found using (5b); 2) since the ferrite medium is assumed to be homogeneous and isotropic, $M_z^{(1)}(\rho,z) = (\mu_r - 1)H_z^{(1)}(\rho,z)$ is easily found from which

$$I_z^*(z) = \mu_0 \int_0^a M_z(\rho,z)\, 2\pi\rho \, d\rho \tag{21}$$

From (5b)

$$H_z^{(1)}(\rho,z) = \frac{1}{i\omega\mu} \left(\frac{\partial E_\phi^{(1)}(\rho,z)}{\partial\rho} + \frac{E_\phi^{(1)}(\rho,z)}{\rho} \right)$$

The substitution for $E_\phi^{(1)}$ from (17) gives

$$H_z^{(1)}(\rho,z) = \frac{aI_0^e}{2\pi} \int_{-\infty}^{\infty} \frac{H_1^{(1)}(\gamma_0 a)}{D(\xi)} \left[\frac{\gamma_1\rho J_1'(\gamma_1\rho) + J_1(\gamma_1\rho)}{\rho} \right] e^{i\xi z} \, d\xi$$

With the identity $xJ_1'(x) + J_1(x) = xJ_0(x)$, this becomes

$$H_z^{(1)}(\rho,z) = \frac{aI_0^e}{2\pi} \int_{-\infty}^{\infty} \frac{H_1^{(1)}(\gamma_0 a)}{D(\xi)} \gamma_1 J_0(\gamma_1\rho) e^{i\xi z} \, d\xi$$

Therefore,

$$M_z^{(1)}(\rho,z) = (\mu_r - 1)H_z^{(1)}(\rho,z)$$

$$= (\mu_r - 1)\frac{aI_0^e}{2\pi}\int_{-\infty}^{\infty}\frac{H_1^{(1)}(\gamma_0 a)}{D(\xi)}\gamma_1 J_0(\gamma_1\rho)e^{i\xi z}\,d\xi$$

The use of this formula for $M_z^{(1)}(\rho,z)$ in (21) yields

$$I_z^*(z) = -i\omega(\mu_r - 1)aI_0^e\mu_0\left[\int_{-\infty}^{\infty}\left(\frac{H_1^{(1)}(\gamma_0 a)}{D(\xi)}e^{i\xi z}\int_0^a J_0(\gamma_1\rho)\gamma_1\rho\,d\rho\right)d\xi\right]$$

Let the variable be changed so that $x = \gamma_1\rho$; then

$$I_z^*(z) = -i\omega(\mu_r - 1)aI_0^e\mu_0\left[\int_{-\infty}^{\infty}\left(\frac{H_1^{(1)}(\gamma_0 a)}{D(\xi)}e^{i\xi z}\frac{1}{\gamma_1}\int_0^{a\gamma_1} xJ_0(x)\,dx\right)d\xi\right] \quad (22)$$

To do the x integral, the following identity is used:

$$xJ_0(x) = xJ_1'(x) + J_1(x) = \frac{d}{dx}[xJ_1(x)]$$

Both sides can be integrated with respect to x:

$$\int xJ_0(x)\,dx = xJ_1(x)$$

Therefore,

$$\int_0^{a\gamma_1} xJ_0(x)\,dx = xJ_1(x)\Big|_0^{a\gamma_1} = a\gamma_1 J_1(\gamma_1 a)$$

When this result is substituted in (22), the following expression is obtained:

$$I_z^*(z) = -i\omega(\mu_r - 1)a^2 I_0^e\mu_0\left[\int_{-\infty}^{\infty}\frac{H_1^{(1)}(\gamma_0 a)J_1(\gamma_1 a)e^{i\xi z}}{a[\gamma_1 J_0(\gamma_1 a)H_1^{(1)}(\gamma_0 a) - \gamma_0\mu_r J_1(\gamma_1 a)H_0^{(1)}(\gamma_0 a)]}\,d\xi\right] \quad (23)$$

Thus, the magnetic current $I_z^*(z)$ (volts) in the ferrite rod is expressed explicitly in an inverse Fourier integral form. The investigation of singularities of the integrand and numerical evaluation of the integral form the subject of Sections VI and VII, respectively.

V. ASYMPTOTIC BEHAVIOR OF THE CURRENT VERY NEAR THE DELTA-FUNCTION GENERATOR

To obtain the behavior near the driving point, the following integral must be evaluated as $z \to 0$:

$$I_z^*(z) \approx -i\omega a(\mu_r - 1)I_0^e\mu_0\left[\int_{-\infty}^{\infty} \frac{aH_1^{(1)}(\gamma_0 a)J_1(\gamma_1 a)}{D(\xi)}\, e^{i\xi z}\, d\xi\right]$$

This is more easily accomplished in the transformed space of ξ. The Fourier transformed current

$$\bar{I}(\xi) \approx -i\omega a(\mu_r - 1)I_0^e\mu_0 \frac{2\pi a H_1^{(1)}(\gamma_0 a)J_1(\gamma_1 a)}{D(\xi)}$$

can be evaluated as $\xi \to \infty$, which is equivalent to looking at $z \to 0$.

$$\left.\bar{I}(\xi)\right\}_{\xi \to \infty} = \lim_{\xi \to \infty}\left[\frac{-i\omega a^2 2\pi\mu_0 I_0^e(\mu_r - 1)H_1^{(1)}(\gamma_0 a)J_1(\gamma_1 a)}{D(\xi)}\right]$$

$$\gamma_1 = \sqrt{k_1^2 - \xi^2} = i\sqrt{\xi^2 - k_1^2} \quad ; \quad \gamma_0 = \sqrt{k_0^2 - \xi^2} = i\sqrt{\xi^2 - k_0^2}$$

As $\xi \to \infty$, $\gamma_1 \to i\xi$ and $\gamma_0 \to i\xi$.

$$\left.\bar{I}(\xi)\right\}_{\xi \to \infty} = \lim_{\xi \to \infty}\left[\frac{-i\omega a^2 2\pi\mu_0(\mu_r - 1)I_0^e H_1^{(1)}(ia\xi)J_1(ia\xi)}{ia\xi J_0(ia\xi)H_1^{(1)}(ia\xi) - \mu_r ia\xi J_1(ia\xi)H_0^{(1)}(ia\xi)}\right]$$

With the use of the modified Bessel functions:

$$J_0(ix) = I_0(x) \quad ; \quad H_1^{(1)}(ix) = -\frac{2}{\pi}K_1(x)$$

$$J_1(ix) = iI_1(x) \quad ; \quad H_0^{(1)}(ix) = -\frac{2i}{\pi}K_0(x)$$

$$\left.\bar{I}(\xi)\right\}_{\xi \to \infty} = \lim_{\xi \to \infty}\left[\frac{-\mu_0 2\pi i\omega I_0^e(\mu_r - 1)a^2(-2/\pi)K_1(a\xi)iI_1(a\xi)}{ia\xi I_0(a\xi)(-2/\pi)K_1(a\xi) - \mu_r ia\xi iI_1(a\xi)(-2i/\pi)K_0(a\xi)}\right]$$

$$= \lim_{\xi \to \infty} \left[\frac{-\mu_0 2\pi i\omega I_0^e(\mu_r - 1)a^2 K_1(a\xi) I_1(a\xi)}{a\xi I_0(a\xi)K_1(a\xi) + \mu_r a\xi I_1(a\xi)K_0(a\xi)} \right]$$

With the use of the asymptotic expansions,

$$\text{as } x \to \infty \quad \begin{cases} K_1(x) \simeq \sqrt{\pi/2x}\; e^{-x} \\ K_0(x) \simeq \sqrt{\pi/2x}\; e^{-x} \\ I_1(x) \simeq \sqrt{1/2\pi x}\; e^{x} \\ I_0(x) \simeq \sqrt{1/2\pi x}\; e^{x} \end{cases}$$

$$\left.\bar{I}(\xi)\right\}_{\xi \to \infty} \simeq -2\pi i\omega I_0^e(\mu_r - 1)\mu_0 a^2 \left(\frac{\frac{1}{2a\xi}}{\frac{1}{2} + \frac{\mu_r}{2}} \right)$$

$$\simeq -2\pi i\omega a I_0^e \mu_0 \frac{\mu_r - 1}{\mu_r + 1} \frac{1}{\xi}$$

Since the current on the antenna is an even function of z, one can write ξ in the foregoing expression as $|\xi|$ and take its cosine inverse transform to get $I_z^*(z)$ as $z \to 0$. Thus,

$$\left. I_z^*(z)\right\}_{z \to 0} = -i4a\omega I_0^e \mu_0 \frac{\mu_r - 1}{\mu_r + 1} \ln |z| + \text{finite integrals} \tag{24}$$

This equation states that the magnetic current has a logarithmic singularity at the source and is similar to the isolated dipole antenna in free space obtained by Wu and King [12].

VI. TRANSMISSION AND RADIATION CURRENTS ON THE ANTENNA

To evaluate the following integral, the singularities of the integrand must be investigated:

$$I_z^*(z) = -i\omega\mu_0(\mu_r - 1)I_0^e \int_{-\infty}^{\infty} \frac{aH_1^{(1)}(\gamma_0 a)J_1(\gamma_1 a)}{D(\xi)} e^{i\xi z}\, d\xi \tag{25}$$

with $D(\xi) = \gamma_1 aJ_0(\gamma_1 a)H_1^{(1)}(\gamma_0 a) - \mu_r\gamma_0 aJ_1(\gamma_1 a)H_0^{(1)}(\gamma_0 a)$ where $\gamma_1 = \sqrt{k_1^2 - \xi^2}$ and $\gamma_0 = \sqrt{k_0^2 - \xi^2}$.

The total magnetic current $I_z^*(z)$ can be thought of as a sum of a transmission current $I_T^*(z)$ and a radiation current $I_R^*(z)$. The contribution from a simple pole gives rise to the transmission current and is associated with a surface wave on the antenna whereas the contribution from the branch cut is correspondingly the radiation current that maintains the electromagnetic fields at distant points.

Note that $\xi = \pm k_1$ are not branch points since the integrand remains unchanged upon adding π to the argument of γ_1. Thus, $\xi = \pm k_0$ are the only branch points. The poles of the integrand can be determined by solving $D(\xi) = 0$, which will be discussed in detail with reference to Fig. 4. This figure shows the path of integration, the pole location and the branch cuts in the complex ξ plane. At this stage, for illustrative purposes, μ_r and ϵ_r are assumed real.

a) On the real axis, for $k_1 < |\xi| < \infty$, with $\alpha = \sqrt{\xi^2 - k_1^2} = -i\gamma_1$ and $\beta = \sqrt{\xi^2 - k_0^2} = -i\gamma_0$; $D(\xi) = i\alpha aJ_0(i\alpha a)H_1^{(1)}(i\beta a) - \mu_r i\beta aJ_1(i\alpha a)H_0^{(1)}(i\beta a)$. Introducing modified Bessel functions, $D(\xi) = 0$ requires that $[\alpha aI_0(\alpha a)K_1(\beta a) + \mu_r\beta aI_1(\alpha a)K_0(\beta a)]$ be equal to zero. Since for real and positive values of α and β, the modified Bessel functions I_0, I_1, K_0 and K_1 are all real and positive, this requirement cannot be met and hence no pole can exist on this part of the real axis.

b) On the part of the real axis where $0 < |\xi| < k_0$ and on the entire imaginary axis, $D(\xi) = 0$ requires that

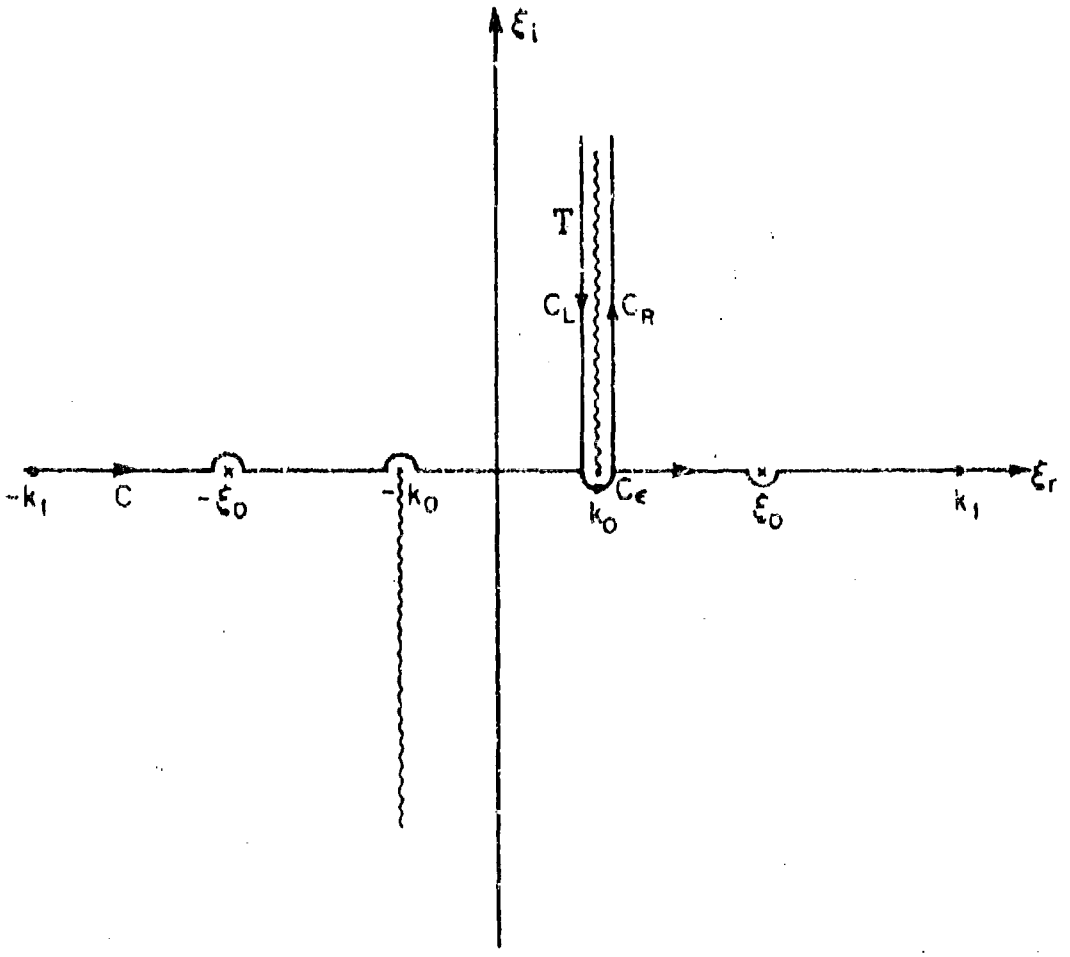

FIG. 4 COMPLEX ξ-PLANE SHOWING THE SINGULARITIES AND THE PATH OF INTEGRATION

$$\frac{\gamma_1 a J_0(\gamma_1 a)}{\mu_r \gamma_0 a J_1(\gamma_1 a)} = \frac{H_0^{(1)}(\gamma_0 a)}{H_1^{(1)}(\gamma_0 a)}$$

$$= \frac{J_0(\gamma_0 a) J_1(\gamma_1 a)}{J_1^2(\gamma_0 a) + Y_1^2(\gamma_0 a)} + i \frac{J_1(\gamma_0 a) Y_0(\gamma_0 a) - J_0(\gamma_0 a) Y_1(\gamma_0 a)}{J_1^2(\gamma_0 a) + Y_1^2(\gamma_0 a)}$$

The left-hand side of the above equation is always real for the range of ξ values being considered whereas for the right-hand side to be real $J_0(\gamma_0 a) Y_0'(\gamma_0 a) - Y_0(\gamma_0 a) J_0'(\gamma_0 a)$ should be equal to zero. But this is a Wronskian and cannot be equal to zero. Therefore, there is no pole on the part of the real axis for $0 < |\xi| < k_0$ or on the entire imaginary axis.

c) On the real axis, for $k_0 < |\xi| < k_1$, the equation $D(\xi) = 0$ becomes

$$\gamma_1 a J_0(\gamma_1 a) H_1^{(1)}(i\beta a) - \mu_r i\beta a J_1(\gamma_1 a) H_0^{(1)}(i\beta a) = 0$$

or (26)

$$\gamma_1 a J_0(\gamma_1 a) K_1(\beta a) + \mu_r \beta a J_1(\gamma_1 a) K_0(\beta a) = 0$$

$$-y J_0(y)/J_1(y) = \mu_r x K_0(x)/K_1(x) \tag{27}$$

where x and y are both positive and real with $x = \beta a$ and $y = \gamma_1 a$. The transcendental equation (27) is similar to the one obtained by Sommerfeld [18] in the problem of waves on wires. However, the graphical method used here for solving the equation is essentially the same as that of Duncan [8]. Since the right-hand side of (27) is always positive and real for lossless ferrite medium, a solution is possible only when y is such that $J_0(y)$ and $J_1(y)$ carry opposite signs. This can also be observed in Fig. 5 and leads to

$$y_{0,i} < a\sqrt{k_1^2 - \xi_0^2} < y_{1,(i+1)} \quad \text{for } i = 1, 2, \ldots \tag{28}$$

where ξ_0 is the solution, i.e., $D(\pm\xi_0) = 0$.

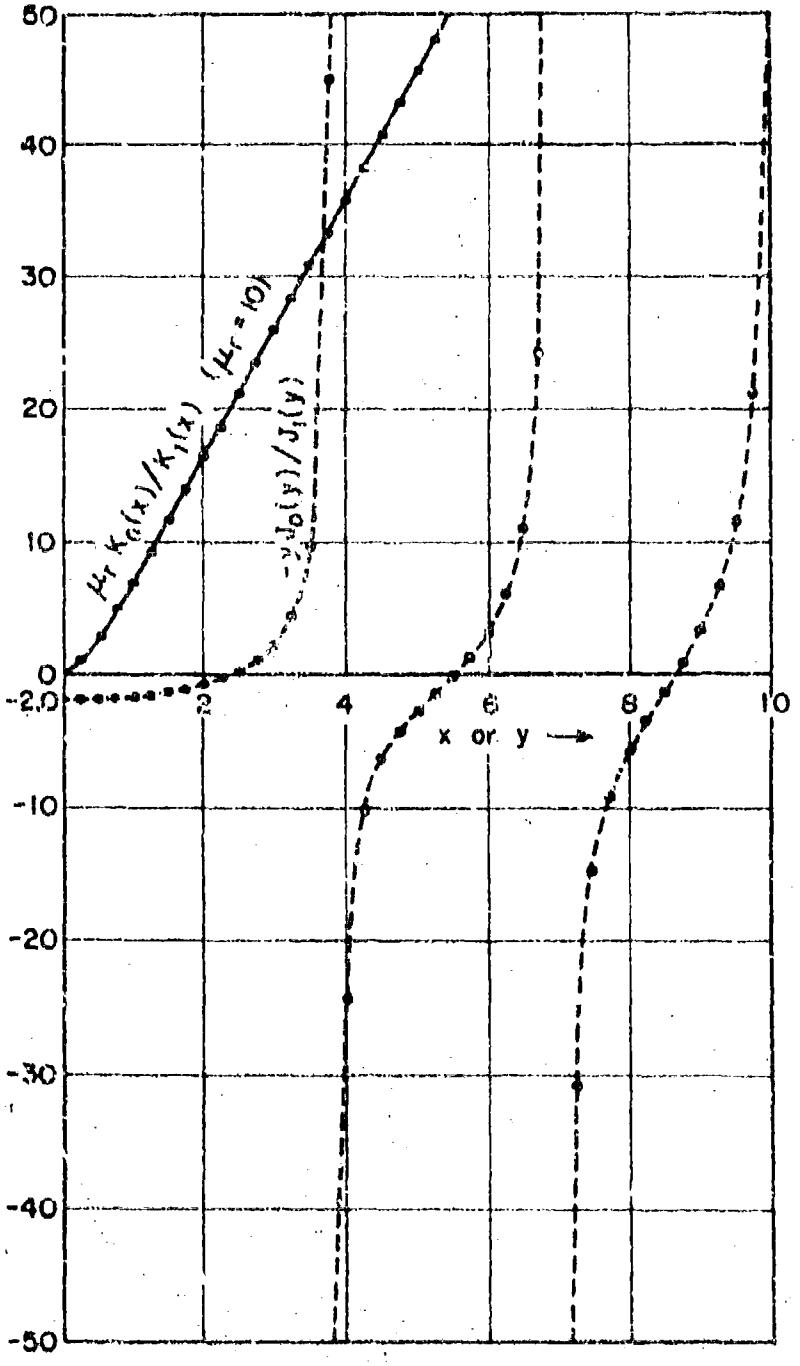

FIG. 5 GRAPHICAL SOLUTION FOR TRANSCENDENTAL EQN (26)

$y_{0,i}$ = i^{th} zero of $J_0(y)$

$y_{1,(i+1)}$ = $(i+1)^{th}$ zero of $J_1(y)$;

for example,

$y_{0,1} = 2.405$	$y_{1,2} = 3.835$
$y_{0,2} = 5.520$	$y_{1,3} = 7.015$
$y_{0,3} = 8.654$	$y_{1,4} = 10.174$

From Fig. 5 it is also clear that for every value of x there are infinite values of y which satisfy the transcendental equation (27). Each of these solutions corresponds to a rotationally symmetrical TE propagating mode on the antenna. Fig. 6 illustrates the multi-valued nature of y, arising out of the infinite branches of the left-hand side of equation (27). Each point (x,y) on the dashed curves in Fig. 6 leads to a possible solution $\pm\xi_0$. Also, $x = a\sqrt{\xi^2 - k_0^2}$ and $y = a\sqrt{k_1^2 - \xi^2}$ which leads to

$$x^2 + y^2 = R^2 \tag{29}$$

where $R^2 = (ak_0)^2(\mu_r\epsilon_r - 1)$.

Since x and y have to satisfy equations (27) and (29) simultaneously, there are now a finite number of solutions as exemplified by the circle C_3. If R is such that $2.405 < R < 5.520$, only the dominant TE mode is supported by the ferrite rod. If $R < 2.405$ like on C_1, the antenna is below cut-off for all the propagating surface modes. Furthermore, for practical ferrites since $\mu_r\epsilon_r >> 1$, $R \simeq ak_1$. Thus, one can reach a conclusion that ak_1 has to be at least 2.405 for the surface waves to appear and additional modes are supported if μ_r is increased sufficiently. Also, when a surface wave is

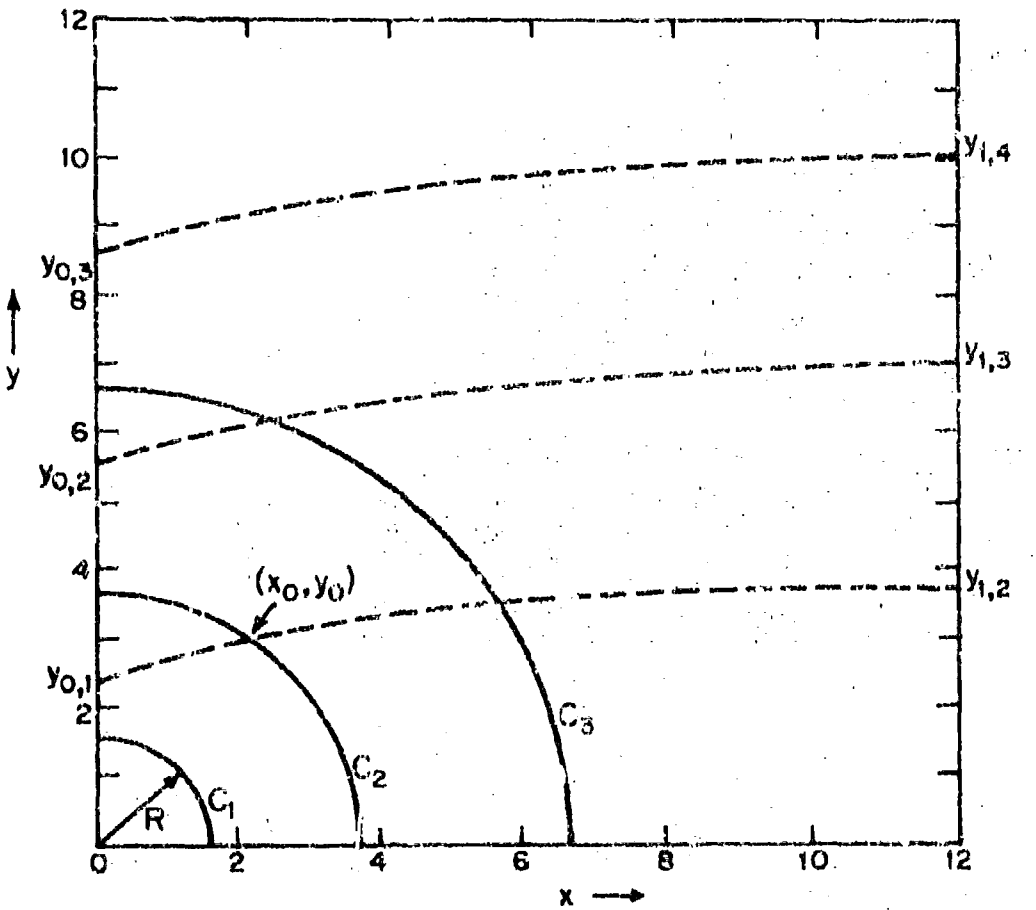

FIG. 6 GRAPHICAL SOLUTION FOR SURFACE WAVE PROPAGATION CONSTANT ξ_0

present, its propagation constant ξ_0 will lie between the wave numbers k_0 and k_1 of free space and the ferrite medium, respectively.

d) It still remains to examine the finite complex ξ plane for the solutions of the equation $D(\xi) = 0$. Since no analytic solution is possible, numerical procedure consisted of computing the magnitude of the reciprocal of $D(\xi)$ at several grid points in a square of size $2k_1$ in the first quadrant of the complex ξ plane. This computation was carried out on both the Reimann sheets of the complex integrand of (23) for $\mu_r = \epsilon_r = 10.0$ and $ak_0 = 0.05$. A solution to $D(\xi) = 0$ is identified with a peaked behavior of increasing amplitude in $|1/D(\xi)|$. The real axis solution $\pm\xi_0$ of c) with $k_0 < |\xi_0| < k_1$ was found within computational accuracy and no other solution could be found. Although this is not a conclusive search for the roots of $D(\xi) = 0$, it should be pointed out that the solutions, if any, in the lower half plane, leading to growing waves, are to be discarded. Furthermore, any solution away from the real axis in the upper half of the complex ξ plane gives rise to rapidly attenuating surface waves which are significant only at very short distances from the delta-function generator.

Returning to the integral of equation (23), the original path of integration C, which runs along the real axis with suitable indentations, can be deformed and shown equivalent to the contour Γ if the pole contribution at $\xi = \xi_0$ is suitably taken into account (see Appendix II).

The total magnetic current $I_z^*(z)$ can now be written as

$$I_z^*(z) = I_T^*(z) + I_R^*(z)$$

with

$$I_T^*(z) = 2\pi i \left\{ \frac{-i\omega a^2 \mu_0(\mu_r - 1)\gamma_0^2 H_1^{(1)}(\gamma_0 a) J_1(\gamma_1 a) e^{i\xi z}}{\frac{d}{d\xi}\left[\gamma_1 a J_0(\gamma_1 a) H_1^{(1)}(\gamma_0 a) - \mu_r \gamma_0 a J_1(\gamma_1 a) H_0^{(1)}(\gamma_0 a)\right]} \right\}_{\xi = \xi_0} \tag{20}$$

and

$$I_R^*(z) = -i\omega\mu_0(\mu_r - 1)I_0^e \int_\Gamma \frac{aH_1^{(1)}(\gamma_0 a)J_1(\gamma_1 a)}{D(\xi)} e^{i\xi z}\, d\xi \tag{31}$$

The contour Γ as shown in Fig. 4 consists of paths C_L and C_R which run to the left and right of the branch cut and also C_ε which is a semi-circular path around the branch tip. It can be shown that the contribution at the tip is vanishingly small which leaves only sections C_L and C_R to be computed.

Let the variable be changed so that $\xi = k_0(1 + ye^{i\theta})$.

$$\text{On } C_L\ ,\ \xi = \xi_L = k_0(1 + ye^{-i3\pi/2}) \tag{32a}$$

$$\text{On } C_R\ ,\ \xi = \xi_R = k_0(1 + ye^{i\pi/2}) \tag{32b}$$

Therefore,

$$I_R^*(z) = -i\omega\mu_0(\mu_r - 1)I_0^e\left[\int_0^\infty \bar{I}(\xi_R)e^{i\xi_R z}\, dy - \int_0^\infty \bar{I}(\xi_L)e^{i\xi_L z}\, dy\right] \tag{33}$$

where

$$\bar{I}(\xi_R) = aH_1^{(1)}\left(a\sqrt{k_0^2 - \xi_R^2}\right) J_1\left(a\sqrt{k_1^2 - \xi_R^2}\right)/D(\xi_R)$$

and

$$\bar{I}(\xi_L) = aH_1^{(1)}\left(a\sqrt{k_0^2 - \xi_L^2}\right) J_1\left(a\sqrt{k_1^2 - \xi_L^2}\right)/D(\xi_L)$$

Substituting for ξ_R and ξ_L from (32) into the above and using the analytic continuation properties of Bessel and Hankel functions, one obtains

$$\bar{I}(\xi_L) = aH_1^{(1)}(v)J_1(u)/A(u,v) \tag{34a}$$

$$\bar{I}(\xi_R) = aH_1^{(2)}(v)J_1(u)/B(u,v) \tag{34b}$$

where

$$A(u,v) = uJ_0(u)H_1^{(1)}(v) - \mu_r vJ_1(u)H_0^{(1)}(v) \tag{35a}$$

$$B(u,v) = uJ_0(u)H_1^{(2)}(v) - \mu_r vJ_1(u)H_0^{(2)}(v) \tag{35b}$$

and

$$u = ak_0\sqrt{\mu_r\epsilon_r - (1 + iy)^2} \tag{36a}$$

$$v = ak_0\sqrt{1 - (1 + iy)^2} \tag{36b}$$

Upon using (32) and (34), the two integrals in (33) can be combined to yield

$$I_R^*(z) = \frac{-4i}{\pi}\,\zeta_0 I_0^e \mu_r(\mu_r - 1)(ak_0)^2 e^{ik_0 z}\int_0^\infty \frac{J_1^2(u)}{A(u,v)B(u,v)}\,e^{-yk_0 z}\,dy \tag{37}$$

where $\zeta_0 = 120\pi$ ohms is the free space characteristic impedance; $A(u,v)$, $B(u,v)$ and u,v are defined in (35) and (36), respectively.

VII. NUMERICAL COMPUTATION

A. Radiation Part of Magnetic Current

In order to compute numerically $I_R^*(z)$ from (37), it is useful to examine the nature of the integrand. Equation (37) is rewritten as follows:

$$I_R^*(z) = \frac{-4i}{\pi}\,\zeta_0 I_0^e \mu_r(\mu_r - 1)(ak_0)^2 e^{ik_0 z}\int_0^\infty f(y)e^{-yk_0 z}\,dy \tag{38}$$

The integrand with the factor $\exp(-yk_0 z)$ suppressed is given by

$$f(y) = f_r(y) + if_i(y) = J_1^2(u)/A(u,v)B(u,v)$$

$$= J_1^2(u)/[uJ_0(u)H_1^{(1)}(v) - \mu_r vJ_1(u)H_0^{(1)}(v)][uJ_0(u)H_1^{(2)}(v) - \mu_r vJ_1(u)H_0^{(2)}(v)] \tag{39}$$

with

$$u = ak_0\sqrt{\mu_r\epsilon_r - (1 + iy)^2} \quad \text{and} \quad v = ak_0\sqrt{1 - (1 + iy)^2}$$

Fortran IV subroutines are now required to compute J_0, J_1, $H_0^{(1)}$, $H_0^{(2)}$, $H_1^{(1)}$ and $H_1^{(2)}$ for complex arguments in order to obtain $f(y)$. Subroutine

BSLSML (of Bhat [13]) has been modified for double precision accuracy. This program uses the series expansion for $J_n(z)$

$$J_n(z) = \sum_{m=0}^{\infty} \frac{(-1)^m}{m!(m+n)!} (z/2)^{2m+n}$$

Knowing the argument z and order n, the total number of terms in the series representation required to achieve a preassigned accuracy is easily determined by solving a quadratic equation. Then use is made of Horner's algorithm by casting the finite series in the form $(z(z(z + a) + b) + c)\ldots$ and the products are computed from the innermost to outermost, thus minimizing the round-off errors. For large arguments ($|z| > 20$), the asymptotic expansion is used.

Subroutine BESH computes the Hankel functions $H_0^{(1)}$, $H_0^{(2)}$, $H_1^{(1)}$ and $H_1^{(2)}$ for complex argument z with double precision accuracy. It makes use of the program 'BESK' from the OS/360 IBM Scientific Subroutine package which was modified by Bhat [13] for complex arguments. 'BESK' computes the modified Bessel function $K_0(z)$ and $K_1(z)$ which are then used in computing the Hankel functions. BSLSML and BESH were both tested and checked against the National Bureau of Standards Tables [14],[15] for J_0, J_1, Y_0 and Y_1 of a complex argument $\rho e^{i\phi}$. From these tables, Hankel functions are calculated using the following relationships for n = 0 and 1,

$$H_n^{(1)}(z) = J_n(z) + iY_n(z)$$

$$H_n^{(2)}(z) = J_n(z) - iY_n(z)$$

With complex double precision, an accuracy of at least 5 significant digits was obtained for both the subroutines when $0 < \rho < 20$ and $0 \leq \phi \leq 180°$. Because of the multiplying factor $\exp(-yk_0z)$, both the real and imaginary

parts of the total integrand are rapidly decaying functions of y and it was found that f_r and f_i need be calculated for y ranging from 0 to 50 only.

In the expression (39) for f(y) u and v are the complex arguments of Bessel and Hankel functions, respectively. With the maximum value of y near 50 and for the range of values of ak_0, μ_r and ϵ_r considered, $|u|$ and $|v|$ do not exceed 15 and 10, respectively. This ensures that the subroutines BSLSML and BESH are used well within the range of their validity.

i) f(y) as a function of y, and the numerical integration for the radiation current:

In this section the behavior of the real and imaginary parts f_r and f_i of f(y) [which can now be calculated using BESH and BSLSML] is discussed. The dielectric constant ϵ_r of the ferrite medium is held constant at 10.0. Two values of electrical radii, viz., ak_0 = 0.05 and 0.1, are considered. For each ak_0 the relative permeability μ_r is varied over a range of values extending from 10 to 200. f_r and f_i are shown graphically in Figs. 7 and 8.

For the rod with the smaller radius, f_r and f_i have, respectively, a positive and negative peak (Fig. 7) initially, but as μ_r is increased their roles are reversed. A somewhat similar behavior is found for the larger radius (Fig. 8). Furthermore, in either case, both f_r and f_i tend asymptotically to zero for large values of y. The decay of both the real and imaginary parts of the total integrand $[f(y)\exp(-yk_0z)]$ is even faster because of the multiplicative real exponential factor. Due to this, a preliminary evaluation of the integral of equation (38) showed that the upper limit of integration can be replaced by 20 or less without any significant loss in accuracy. It is important to perform the integration accurately around the peak because of its significant contribution to the total integral. A 12-point Gauss quadrature routine from OS/360 IBM Scientific Subroutine package has

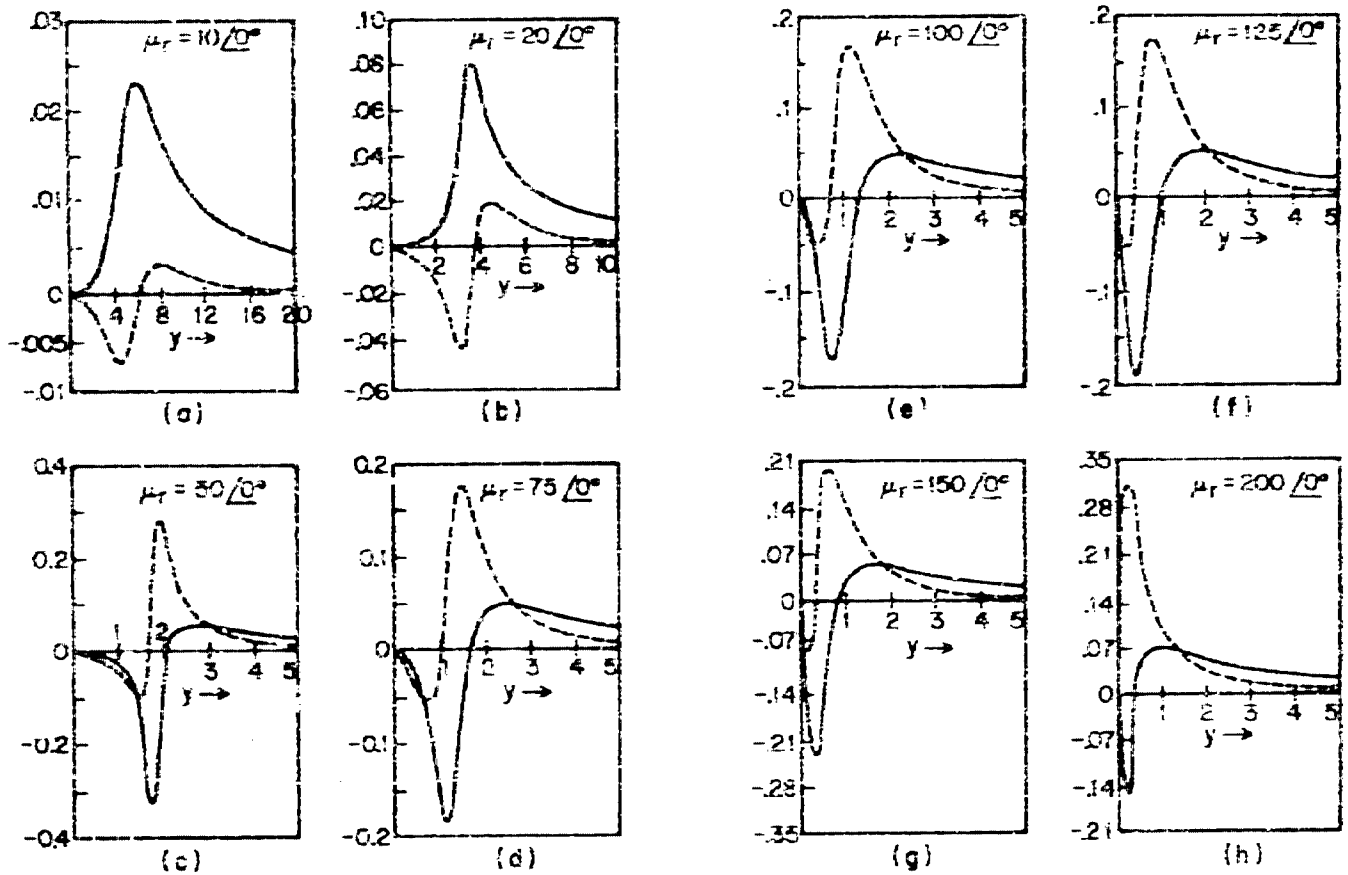

FIG. 7 REAL AND IMAGINARY PARTS OF f(y) [THE INTEGRAND WITH EXP($-jk_0z$) SUPPRESSED] AS A FUNCTION OF y FOR VARYING μ_r: $ak_0 = .05$, $\epsilon_r = 10.0$: ----Im[f(y)], ——Re[f(y)]

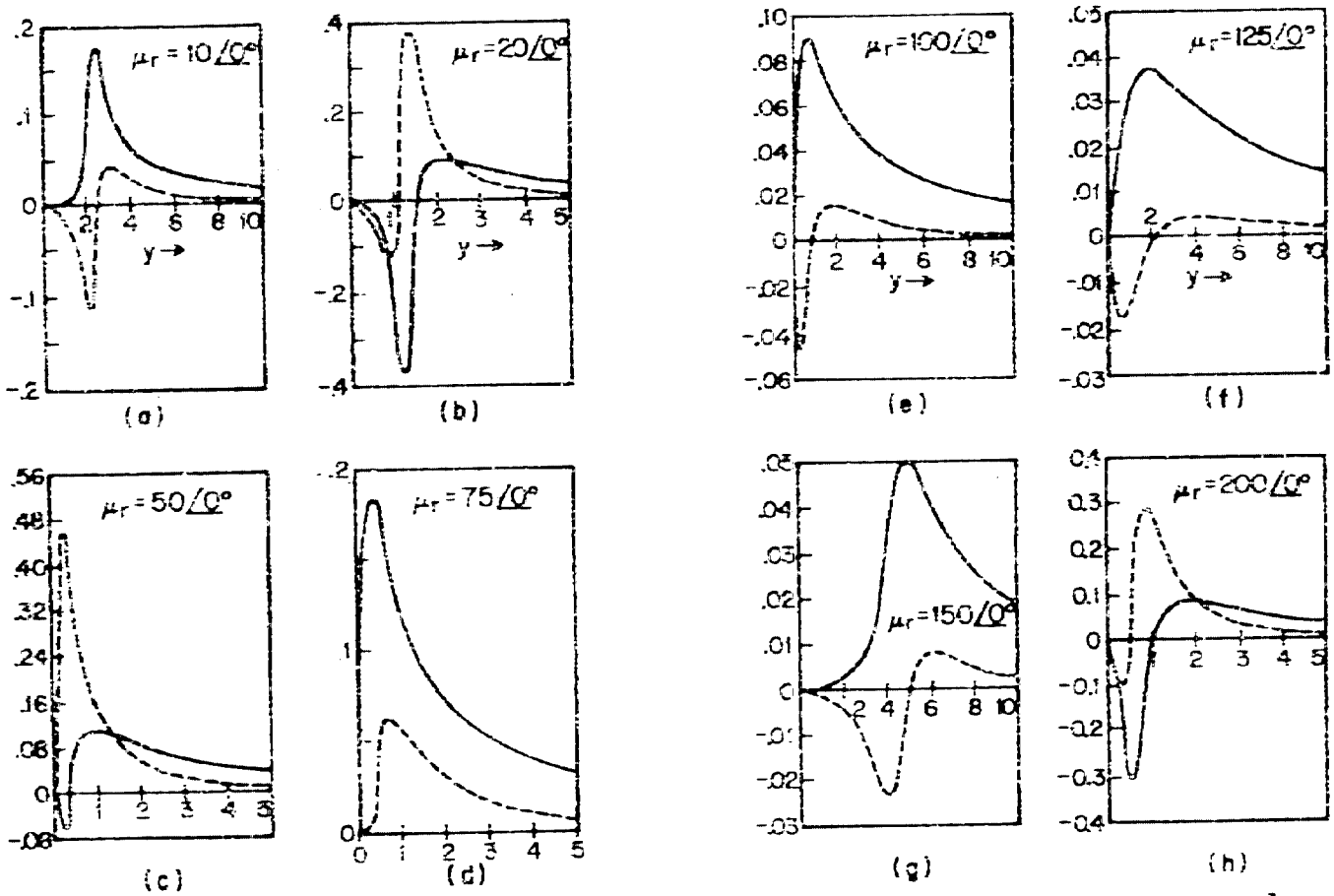

FIG. 8 REAL AND IMAGINARY PARTS OF f(y) [THE INTEGRAND WITH EXP($-jk_0z$) SUPPRESSED] AS A FUNCTION OF y FOR VARYING μ_r; $ak_0 = 0.1$, $\epsilon_r = 10.0$: ---- Im[f(y)], —— Re[f(y)]

been used [16]. In order to meet a specified convergence criterion, the total range of integration was divided into sufficient number of panels, not to exceed 5 in any case. Since the integrand has been previously calculated and plotted (Figs. 7 and 8), the location of the peaks in both the real and imaginary parts are accurately known. Panels are of unequal width and are more closely spaced around the peak. The optimum number of panels M is decided by requiring that the value of the integral using M and (M + 1) divisions differ by less than 10^{-4} in magnitude. The results of these computations are shown graphically in Figs. 10 and 11; they are discussed in Section VIII.

B. Transmission Part of Magnetic Current

The transmission current on the antenna is given by the contribution of the residue at the pole $\xi = \xi_0$, to the integral of equation (25). This was calculated in (30) to be

$$\frac{I_T^*(z)}{I_0^e}\ (\text{volts/amp}) = 2\pi i \left\{ \frac{-i\omega a^2 \mu_0(\mu_r - 1) H_1^{(1)}(\gamma_0 a) J_1(\gamma_1 a) e^{i\xi z}}{\frac{d}{d\xi}[D(\xi)]} \right\}_{\xi=\xi_0} \tag{40}$$

The location of the pole $\xi = \xi_0$ was briefly discussed in Section VI. It is now useful to set up a graphical procedure to determine ξ_0 and carry out a sample calculation for the case of real parameters μ_r and ϵ_r. Fig. 9(a) shows the electrical radius ak_0 as a function of frequency ranging from 1 to 1000 MHz. Practical values of the diameter of the ferrite rod are considered and it ranges from 1/2" to 4". In an actual experimental setup, care must be taken to ensure the validity of the constant current approximation in the driving loop by requiring $ak_0 < 0.1$. Having determined ak_0 and knowing μ_r and ϵ_r, one can obtain the value of the parameter R which then is plotted in Fig. 9(c) as illustrated. A knowledge of x_0 from Fig. 9(c) is used in 9(d)

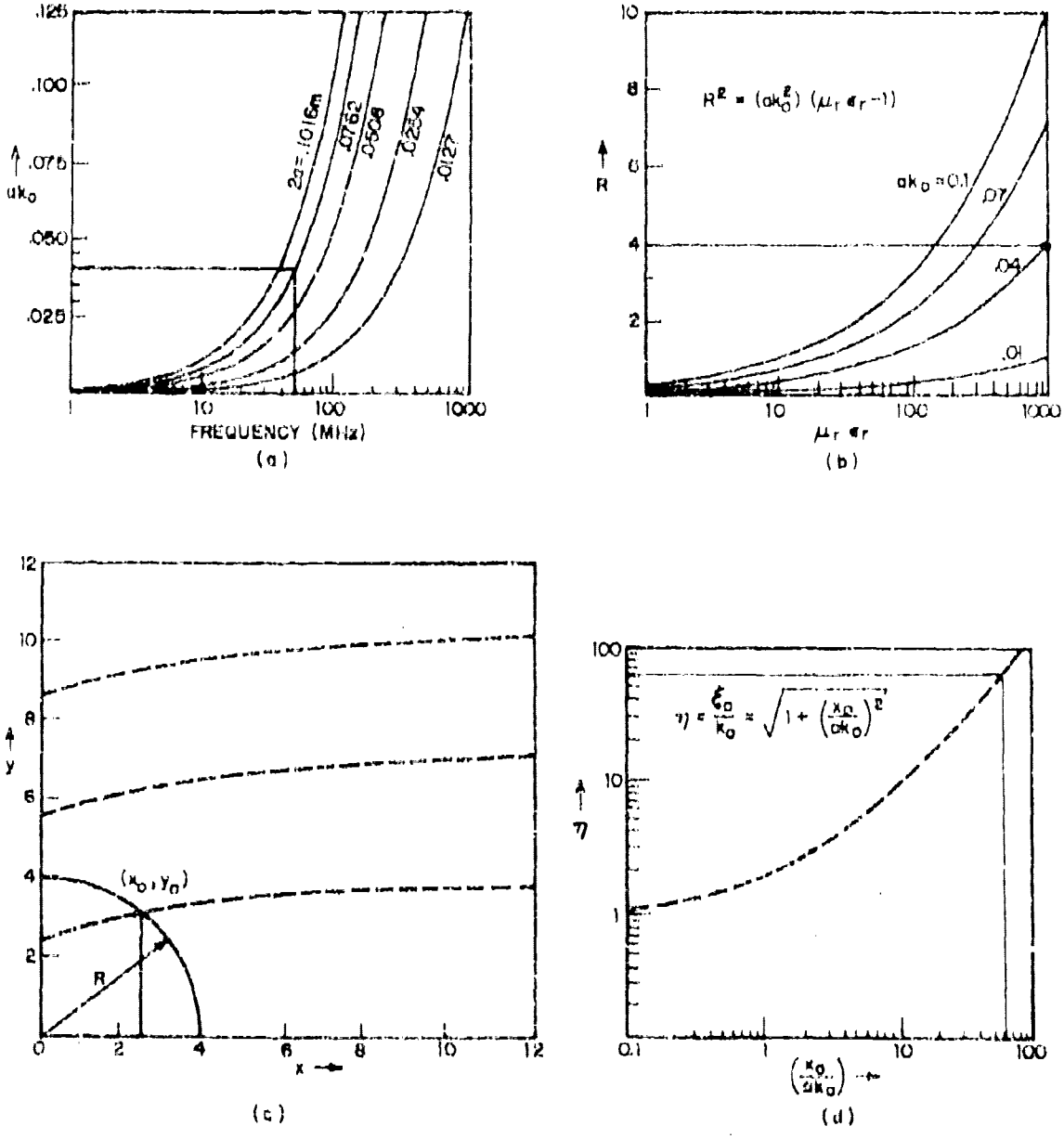

FIG. 9 GRAPHIC PROCEDURE TO DETERMINE THE NORMALIZED PROPAGATION CONSTANT (ξ_0/x_0) OF THE DOMINANT TE MODE

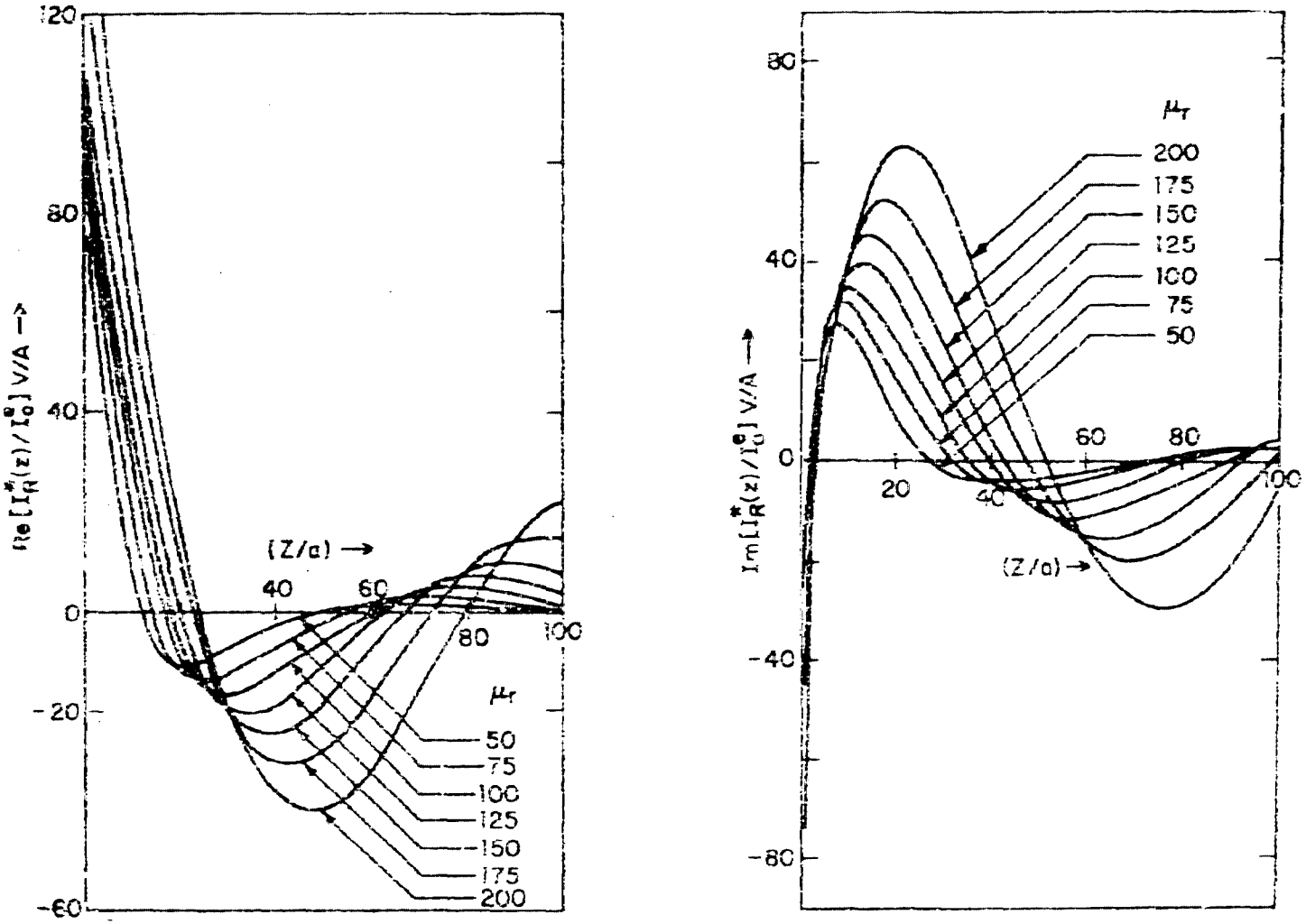

FIG. 10 REAL AND IMAGINARY PARTS OF NORMALIZED RADIATION CURRENT AS A FUNCTION OF NORMALIZED DISTANCE FOR VARYING VALUES OF μ_r; $\epsilon_r = 10.0$, $ak_0 = 0.05$.

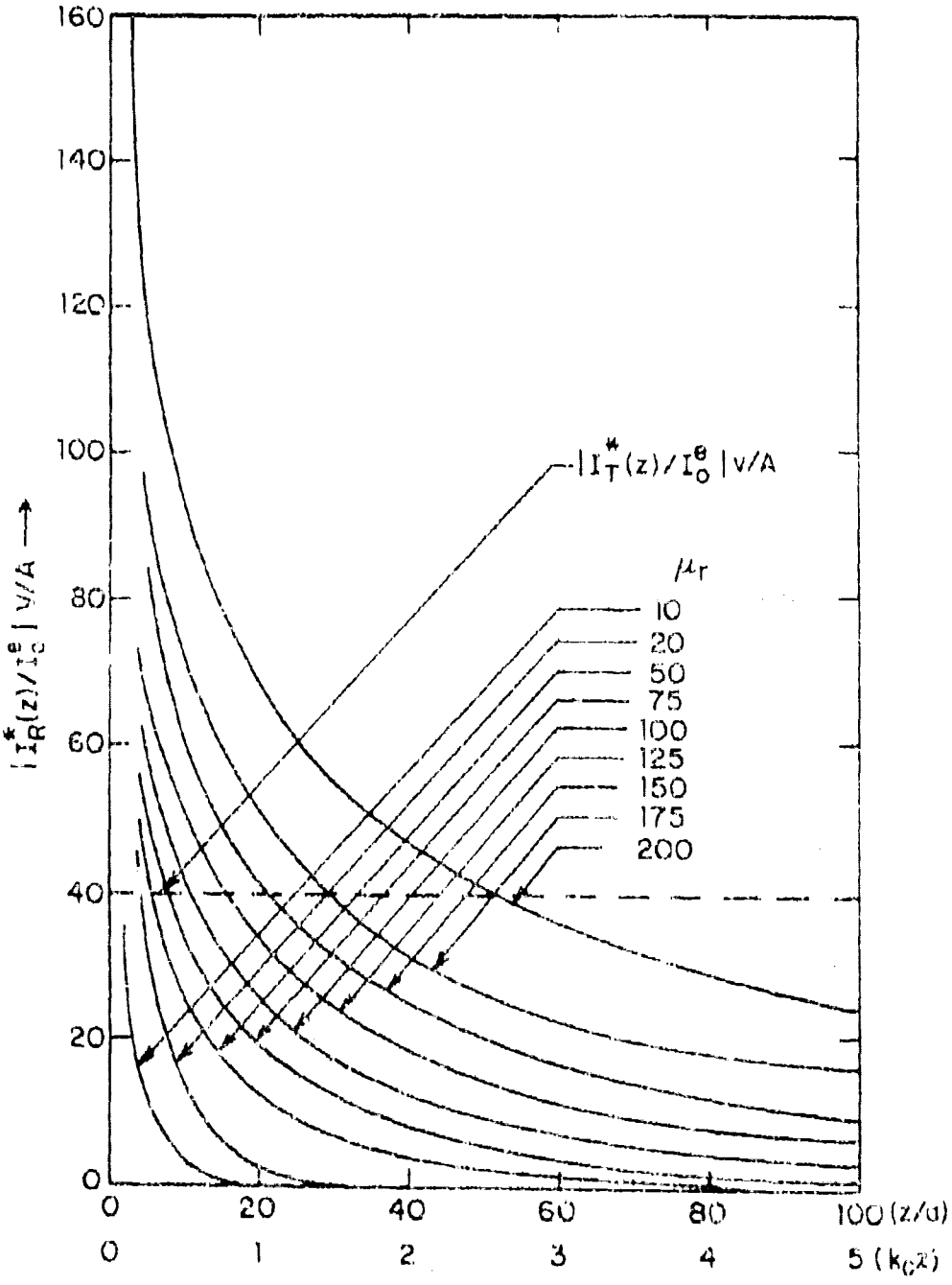

FIG. 11 MAGNITUDE OF THE NORMALIZED RADIATION CURRENT AS A FUNCTION OF NORMALIZED DISTANCE FOR VARYING VALUES OF μ_r; $\epsilon_r = 10.0$, $ak_0 = 0.05$. MAGNITUDE OF NORMALIZED TRANSMISSION CURRENT SHOWN BY DOTTED LINE IS FOR $\mu_r = 100.0$, $\epsilon_r = 10.0$ AND $ak_0 = 0.04$

to determine the value of the propagation constant ξ_0 normalized to the free space wave number k_0. Letting $\xi_0/k_0 = \eta$, carrying out the differentiation in the denominator and after simplifying, (40) becomes

$$\frac{I_T^*(z)}{I_0^e}\ (\text{volts/amp}) = \frac{-2\pi\zeta_0 e^{i\eta k_0 z}}{\eta\left[1 + \frac{y_0^2}{\mu_r x_0^2}\frac{J_0^2(y_0)}{J_1^2(y_0)} + \frac{R^2}{x_0^2(\mu_r - 1)}\frac{J_0(y_0)J_2(y_0)}{J_1^2(y_0)}\right]} \tag{41}$$

where $\zeta_0 = 120\pi$ ohms is the free space characteristic impedance and $R = (x_0^2 + y_0^2)^{1/2}$.

The traveling-wave nature of the transmission current can now be seen from (41) so that it is sufficient to plot the magnitude of the normalized current $|I_T^*(z)/I_0^e|$ as a function of the normalized distance.

<u>Example:</u> $\mu_r = 100.0$, $\epsilon_r = 10.0$, $f = 50$ MHz, $2a = 0.0762$ m or 3 in.

i) From Fig. 9(a), $ak_0 = 0.04$

ii) From Fig. 9(b), $R = 4.0$

iii) From Fig. 9(c), $x_0 = 2.50$, $y_0 = 3.12$; thus, $x_0/ak_0 = 62.5$

iv) From Fig. 9(d), $\eta = \xi_0/k_0 = 62.503$

Using the above values in (41) $|I_T^*(z)/I_0^e|$ is found to be 39.05 volts/amp and is shown plotted in Fig. 11.

VIII. SUMMARY

An electrically small loop that carries a constant current and is loaded by an infinitely long, homogeneous, isotropic ferrite rod has been called the ferrite-rod antenna. The ferrite-rod antenna is treated using a boundary-value approach. An explicit expression for the magnetic current in the form of an inverse Fourier integral has been derived and numerically computed. Two values of the electrical radius for the loop are considered. For one of the cases the magnetic current is represented graphically as a function of the

normalized distance for a range of values of the relative permeability of the ferrite rod. The magnetic current is found to consist of a transmission and a radiation part. If μ_r and ϵ_r of the ferrite rod are assumed to be real, then the transmission current can be associated with an unattenuated TE surface wave. This surface wave is rotationally symmetrical and has a cut-off condition. Since this surface wave does not contribute to radiation, the cut-off condition is easily met at frequencies where ferrite-rod antennas are useful in practice and, thus, the propagating surface mode can be made to disappear. The radiation current on the ferrite rod is a decaying function of distance away from the delta-function source. Furthermore, the asymptotic behavior of the magnetic current near the delta-function generator was found to be logarithmic and, hence, similar to the electric current in the dipole antenna (Wu and King [12]). The analogy between the ferrite-rod antenna and the conducting cylindrical dipole antenna was discussed in Section II. It was also mentioned that a comparison of the ferrite-rod antenna with the dielectric rod antenna is possible on the basis of physical mechanisms inside the material. The present formulation can be compared directly with the work of Ting [17] on the dielectric-coated antenna. In this a current distribution which also includes a transmission and a radiation part has been obtained.

The magnetic currents plotted in this report are for ferrite cores of infinite length. However, in practice, low frequency antennas like the ferrite rod are of necessity finite and even electrically short. Therefore, a logical extension of this formulation is to obtain magnetic current distributions on a finite rod. With this current distribution precisely known, in principle, other quantities of interest like the radiated field and radiation efficiency can be derived from it. It is expected that this will form the subject of Part II of this report to be published at a later date.

LIST OF SYMBOLS

(ρ,ϕ,z)	Circular cylindrical coordinates
μ	$= \mu_0(\mu_r' + i\mu_r'')$, permeability of ferrite medium
μ_r	Complex relative permeability
ϵ	$= \epsilon_0(\epsilon_r' + i\epsilon_r'')$, permittivity of ferrite medium
ϵ_r	Complex dielectric constant
σ	Conductivity
I_0^e	Strength of constant current in the driving loop
a	Radius of loop = radius of ferrite rod
ω	Angular frequency
k	$= \omega\sqrt{\mu\epsilon}$, wave number
ζ	Fourier transform variable for z coordinate
$\bar{E}(\rho,\zeta)$	z-transformed electric field
i	$= \sqrt{-1}$
$J_n(x)$	Bessel function of first kind and order n
$Y_n(x)$	Neumann function of order n
$H_n^{(1)}(x)$	Hankel function of first kind and order n
$H_n^{(2)}(x)$	Hankel function of second kind and order n

[Above functions when primed mean derivatives with respect to their arguments]

γ_0	$= \sqrt{k_0^2 - \zeta^2}$
γ_1	$= \sqrt{k_1^2 - \zeta^2}$
(R,ϕ,θ)	Spherical polar coordinates

ACKNOWLEDGMENT

I am grateful to Professors R. W. P. King and T. T. Wu for their valuable advice and suggestions, and to Miss Margaret Owens for her assistance in the preparation of this report.

REFERENCES

[1] S. Adachi, "Impedance Characteristics of a Uniform Current Loop Having a Spherical Ferrite Core," The Ohio State University Research Foundation, Columbus, Ohio, Report No. 662-26, April 15, 1959.

[2] O. R. Cruzan, "Radiation Properties of a Spherical Ferrite Antenna," Diamond Ordnance Fuze Laboratories, Washington, D.C., Tech. Report No. TR-307, October 15, 1956.

[3] J. Dorman, "Thin Wire Loop and Thin Biconical Antennas in Finite Spherical Media," Ph.D. Dissertation, University of Maryland, College Park, Maryland, 1957.

[4] C.-T. Tai, "Radiation from a Uniform Circular Loop Antenna in the Presence of a Sphere," Research Institute, Stanford University, California, Tech. Report No. 32, December 1952.

[5] H. A. Isiaw, "A Theoretical Treatment of Low-Frequency Loop Antennas With Permeable Cores," IEEE Trans. Antennas Propagation, vol. AP-11, No. 3, pp. 152-165, March 1963.

[6] R. W. P. King and T. T. Wu, "The Imperfectly Conducting Cylindrical Transmitting Antenna," IEEE Trans. Antennas Propagation, vol. AP-14, No. 5, pp. 524-534, May 1966.

[7] R. W. P. King, C. W. Harrison, Jr., and E. A. Aronson, "The Imperfectly Conducting Cylindrical Transmitting Antenna: Numerical Results," IEEE Trans. Antennas Propagation, vol. AP-14, No. 5, pp. 535-542, May 1966.

[8] J. W. Duncan, "The Efficiency of Excitation of a Surface Wave on a Dielectric Cylinder," Ph.D. Dissertation, University of Illinois, 1958.

[9] W. Magnus and F. Oberhettinger, Formulas and Theorems for the Special Functions of Mathematical Physics (translated by J. Wermer). New York: Chelsea Publishing Co., 1949. p. 34.

[10] R. W. P. King, The Theory of Linear Antennas. Cambridge, Mass.: Harvard University Press, 1956.

[11] J. R. Wait, Electr[illegible] Radiation from Cylindrical Structures. London: Pergamon Press, 1959, pp. 162-164.

[12] T. T. Wu and R. W. P. King, "Driving-Point and Input Admittances of Linear Antennas," J. Appl. Phys., vol. 30, No. 1, p. 74, 1959.

[13] B. Bhat, "Current Distribution on an Infinite Tubular Antenna in a Cold Collisional Magnetoplasma," Div. of Engrg. and Appl. Phys., Harvard University, Cambridge, Mass., Tech. Report No. 634, May 1972.

[14] Tables of the Bessel Functions $J_0(z)$ and $J_1(z)$ for Complex Arguments. New York: Columbia University Press, 1947.

[15] Tables of the Bessel Functions $Y_0(z)$ and $Y_1(z)$ for Complex Arguments. New York: Columbia University Press, 1950.

[16] V. I. Krylov, Approximate Calculation of Integrals. New York/London: Macmillan, 1962, pp. 100-111 and 337-340.

[17] O.-Y. Ting, "Infinite Cylindrical Dielectric-Coated Antenna," Radio Sci., vol. 2 (N.S.), No. 3, March 1967.

[18] A. Sommerfeld, Electrodynamics. Academic Press, 1964.

APPENDIX I

BOUNDARY CONDITIONS AND EVALUATION OF CONSTANTS IN FIELD EXPRESSIONS

The purpose of this appendix is to evaluate the constants A and B which appeared in equations (10) and (11),

$$E^{(1)}(\rho,\xi) = AJ_1\left(\sqrt{k_1^2 - \xi^2}\,\rho\right) \qquad \text{for } 0 \le \rho \le a$$

$$E^{(2)}(\rho,\xi) = BH_1^{(1)}\left(\sqrt{k_0^2 - \xi^2}\,\rho\right) \qquad \text{for } a \le \rho \le \infty \quad ,$$

by applying the following boundary conditions:

i) $E(\rho,\xi)$ is continuous at $\rho = a$,

ii) $\left[\dfrac{dE^{(2)}}{d\rho} - \dfrac{1}{\mu_r}\dfrac{dE^{(1)}}{d\rho} + \dfrac{E^{(2)}}{a} - \dfrac{E^{(1)}}{a\mu_r}\right]_{\rho=a} = -i\omega\mu_0 I_0^a$.

The first boundary condition gives:

$$AJ_1(\gamma_1 a) - BH_1^{(1)}(\gamma_0 a) = 0 \tag{I-1}$$

The second condition yields:

$$B\gamma_0 H_1^{(1)\prime}(\gamma_0 a) - \frac{A}{\mu_r}\gamma_1 J_1'(\gamma_1 a) + \frac{B}{a}H_1^{(1)}(\gamma_0 a) - \frac{A}{a\mu_r}J_1(\gamma_1 a) = -i\omega\mu_0 I_0^a \tag{I-2}$$

The two equations in matrix form are

$$\begin{bmatrix} J_1(\gamma_1 a) & -H_1^{(1)}(\gamma_0 a) \\ J_1(\gamma_1 a) + a\gamma_1 J_1'(\gamma_1 a) & -[\mu_r H_1^{(1)}(\gamma_0 a) + a\mu_r H_1^{(1)\prime}(\gamma_0 a)] \end{bmatrix} \begin{bmatrix} A \\ B \end{bmatrix} = \begin{bmatrix} 0 \\ i\omega\mu a I_0^a \end{bmatrix}$$

or

$$\begin{bmatrix} a_{11} & a_{12} \\ a_{21} & a_{22} \end{bmatrix} \begin{bmatrix} A \\ B \end{bmatrix} = \begin{bmatrix} 0 \\ i\omega\mu a I_0^a \end{bmatrix} \tag{I-3}$$

A and B can now be written down using Cramer's rule. Thus,

$$A = i\omega\mu a I_0^{(1)} H_1^{(1)}(\gamma_0 a)/\det a_{ij} \tag{I-4a}$$

$$B = i\omega\mu a I_0^{(1)} J_1(\gamma_1 a)/\det a_{ij} \tag{I-4b}$$

$\det a_{ij} = D(\xi)$

$$= -J_1(\gamma_1 a)[\mu_r H_1^{(1)}(\gamma_0 a) + a\mu_r\gamma_0 H_1^{(1)\prime}(\gamma_0 a)] + H_1^{(1)}(\gamma_0 a)[J_1(\gamma_1 a) + a\gamma_1 J_1'(\gamma_1 a)]$$

$$D(\xi) = J_1(\gamma_1 a)H_1^{(1)}(\gamma_0 a)(1 - \mu_r) + \gamma_1 a J_1'(\gamma_1 a)H_1^{(1)}(\gamma_0 a) - \mu_r J_1(\gamma_1 a)\gamma_0 a H_1^{(1)\prime}(\gamma_0 a)$$

Consider the identity:

$$xf_\nu'(x) = -\nu f_\nu(x) + xf_{\nu-1}(x)$$

where f is any Bessel function. Therefore,

$$\gamma_1 a J_1'(\gamma_1 a) = -J_1(\gamma_1 a) + \gamma_1 a J_0(\gamma_1 a)$$

$$\gamma_0 a H_1^{(1)\prime}(\gamma_0 a) = -H_1^{(1)}(\gamma_0 a) + \gamma_0 a H_0^{(1)}(\gamma_0 a)$$

The use of these identities gives:

$$D(\xi) = J_1(\gamma_1 a)H_1^{(2)}(\gamma_0 a)(1 - \mu_r) + [-J_1(\gamma_1 a) + \gamma_1 a J_0(\gamma_1 a)]H_1^{(1)}(\gamma_0 a)$$
$$- \mu_r J_1(\gamma_1 a)[-H_1^{(1)}(\gamma_0 a) + \gamma_0 a H_0^{(1)}(\gamma_0 a)]$$

$$= J_1(\gamma_1 a)H_1^{(1)}(\gamma_0 a) - \mu_r J_1(\gamma_1 a)H_1^{(1)}(\gamma_0 a) - J_1(\gamma_1 a)H_1^{(1)}(\gamma_0 a)$$
$$+ a\gamma_1 J_0(\gamma_1 a)H_1^{(1)}(\gamma_0 a) - \gamma_0 a\mu_r J_1(\gamma_1 a)H_0^{(1)}(\gamma_0 a) + \mu_r J_1(\gamma_1 a)H_1^{(1)}(\gamma_0 a)$$

Finally,

$$D(\xi) = a[\gamma_1 J_0(\gamma_1 a)H_1^{(1)}(\gamma_0 a) - \gamma_0\mu_r J_1(\gamma_1 a)H_0^{(1)}(\gamma_0 a)] \tag{I-5}$$

APPENDIX II

THE CONTOUR OF INTEGRATION IN EQUATION (25)

The purpose of this appendix is to simplify the path of integration appearing in (25):

$$I_z^*(z) = -i\omega a u_0(\mu_r - 1) I_0^* \int_{-\infty}^{\infty} \frac{a H_1^{(1)}(\gamma_0 a) J_1(\gamma_1 a)}{D(\xi)} e^{i\xi z}\, d\xi$$

In the above equation the path of integration is the entire real axis and is called the contour C, represented by the path A to N in Fig. 12.

Considering the two closed paths ACMPA and JKLMNOJ,

$$\int_{A \text{ to } H} (\ ) + \int_{HP} (\ ) + \int_{PA} (\ ) = 0 \qquad \text{(II-1)}$$

$$\int_{J \text{ to } N} (\ ) + \int_{NO} (\ ) + \int_{OJ} (\ ) = 2\pi i \text{ (residue at the pole } \xi = \xi_0), \qquad \text{(II-2)}$$

$\int_{PA}(\ )$ and $\int_{NO}(\ )$ are both equal to zero since the integrand is vanishingly small on the huge circle. Using this result in (II-1) and (II-2),

$$\int_{A \text{ to } H} (\ ) + \int_{J \text{ to } N} (\ ) = -\int_{HP} (\ ) - \int_{OJ} (\ ) + 2\pi i \text{ (residue at the pole } \xi = \xi_0)$$

Adding the semi-circular path HIJ to both sides of the above equation, one obtains:

$$\int_{C} (\ ) = \int_{\Gamma} (\ ) + 2\pi i \text{ (residue at the pole } \xi = \xi_0)$$

This is the result used in equations (30) through (33).

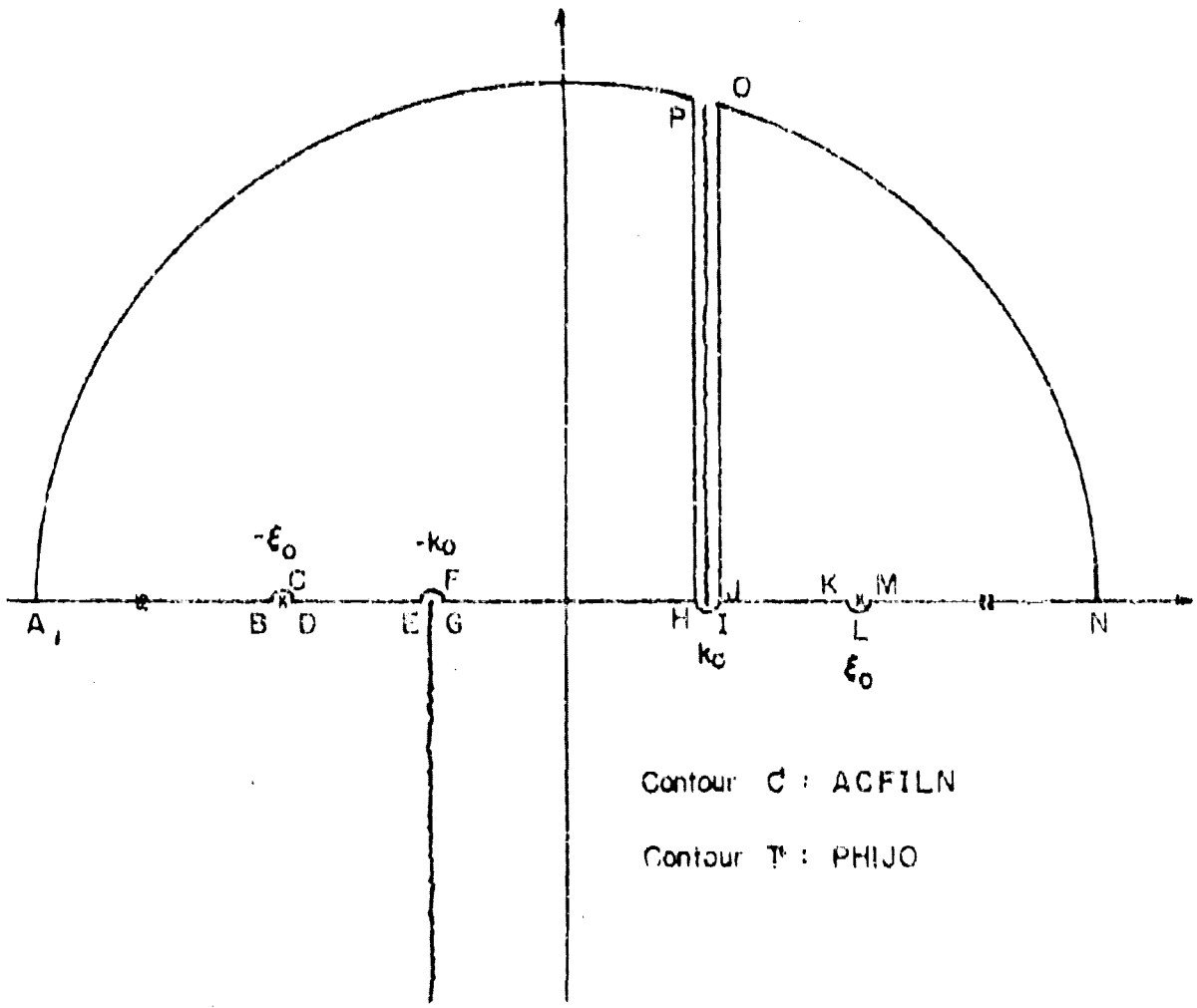

FIG. 12: PATH OF INTEGRATION IN THE COMPLEX ξ-PLANE FOR THE INTEGRAL OF EQN [23]

APPENDIX III

This appendix essentially lists all the Fortran IV programs that were used in the various computations. The 'Main Program' which appears at the beginning was written to compute the radiation part of the magnetic current on the ferrite-rod antenna. Basically it involves a numerical integration of a complex function. For this purpose the behavior of the real and imaginary parts of the integrand for various parameter ranges was examined and a suitable Gaussian Quadrature routine was employed. The numerical evaluation of the integrand itself is comprised of cylindrical functions of complex arguments. Previously available programs [13] were modified to meet the present requirements.

```
C  MAIN PROGRAM
C  THIS FORTRAN-IV PROGRAM COMPUTES THE RADIATION PART OF THE MAGNETIC
C  CURRENT DISTRIBUTION ON AN ELECTRICALLY SMALL LOOP ANTENNA LOADED BY
C  A HOMOGENEOUS AND ISOTROPIC FERRITE CYLINDER OF INFINITE LENGTH.
C
C  FUNCTION SUBPROGRAMS- ' TPR1,TPI '
C  SUBROUTINES- ' GAUSS,OFUN,BESH,BSLSRL,ASY2,ASY3,ASY4,ASY5,ASY6,ASY7 '
C
      IMPLICIT COMPLEX*16(D), REAL*8(T)
      EXTERNAL TPR1,TPI
      COMMON TUR,TER,TKOA,TKOZ
    2 READ (5,5) TUR,TER,TKOA
    5 FORMAT (3(D10.4,1X))
      IF (TUR.GT.999.D0) GO TO 200
      READ (5,10) TL,TU
   10 FORMAT(2(D10.4,1X))
      N=4
      WRITE (6,20)
   20 FORMAT('1',30X,'RADIATION PART OF THE MAGNETIZATION CURRENT ON
     2THE FERRITE ROD ANTENNA './///)
      WRITE (6,30) TUR,TER,TKOA
   30 FORMAT ('0',5X,' RELATIVE PERMEABILITY = ',D10.4,10X,' RELATIVE
     2PERMITIVITY = ',D10.4,10X,'ELECTRICAL RADIUS  KOA = ',D10.4)
      T1=TL
      T2=TU
      TN=DFLOATIN)
      WRITE (6,40)
   40 FORMAT(/,4X,'Z/A',7X,'KOZ',11X,'REAL',10X,'IMAG',19X,'ABS',14X,
     C'PHASE',/)
      TKOZ=TKOA
   42 T3=0.D0
      T4=0.D0
      ZOA=TKOZ/TKOA
      TU=TL+(T2-T1)/TN
   49 CONTINUE
      CALL GAUSS(TL,TU,TPR1,TREA)
      CALL GAUSS(TL,TU,TPI,TIMAG)
      T3=T3+TREA
      T4=T4+TIMAG
      T1=TU
      TU=TU+(T2-T1)/TN
      IF(TU.LE.T2) GO TO 49
      TU=(T2+TU)/2.D0
      TL=T2
      TU=TL+TU
   60 CONTINUE
      CALL GAUSS(TL,TU,TPR1,TREA)
      CALL GAUSS(TL,TU,TPI,TIMAG)
      T3=T3+TREA
      T4=T4+TIMAG
      T1=TU
      TU=TU+TU
      IF (TU.LE.19.D0) GO TO 60
      DI=DCMPLX(T3,T4)
      DI=DI*4D0.D0*(0.D0,1.D0)*CDEXP((0.D0,1.D0)*TKOZ)
      TABS=CDABS(DI)
      TREA=REAL(DI)
      TIMAG=AIMAG(DI)
      TPH=(180.D0/3.141592653589D0)*DATAN2(TIMAG,TREA)
      WRITE (6,50) ZOA,TKOZ,TREA,TIMAG,TABS,TPH
   50 FORMAT (3X,F8.2,2X,D10.4,5X,4(D10.4,8X))
      TL=T1
      TU=T2
      TKOZ=TKOZ+TKOA
      IF (ZOA.LE.99.D1) GO TO 42
      GO TO 2
  200 CONTINUE
      END


C ***********************************************************************
C
C
C  THIS PROGRAM COMPUTES THE INTEGRAL OF F(Y)*EXP(-YK*Z) BETWEEN TWO
C     SPECIFIED LIMITS USING A 12-POINT GAUSS QUADRATURE FORMULA.
C  SINCE F(Y) IS A COMPLEX FUNCTION, THE REAL AND IMAGINARY PARTS ARE
C  INTEGRATED SEPARATELY.
C
      SUBROUTINE GAUSS(TL,TU,TLR,TREAL)
      IMPLICIT REAL*8(T)
      TA=0.5D0*(TU+TL)
      TB=TU-TL
      TC=.49079551712339440D-1*TB
      TREAL=.23507668149232591D-1*(TLR(TA+TC)+TLR(TA-TC))
      TC=.48209862318527465D-1*TB
      TREAL=TREAL+.23469662997459210D-1*(TLR(TA+TC)+TLR(TA-TC))
      TC=.90495133706713234D-1*TB
      TREAL=TREAL+.22003916427167311D-1*(TLR(TA+TC)+TLR(TA-TC))
      TC=.29368847714850107D-1*TB
      TREAL=TREAL+.18153371236133456D-1*(TLR(TA+TC)+TLR(TA-TC))
      TC=.18391374549975810D-1*TB
      TREAL=TREAL+.11674268204917740D-1*(TLR(TA+TC)+TLR(TA-TC))
      TC=.82616706255754450D-1*TB
      TREAL=TB*(TREAL+.12457335590670180D-1*(TLR(TA+TC)+TLR(TA-TC)))
      RETURN
      END
```

```
C  ***********************************************************************
C
C
C  THIS FUNCTION SUBPROGRAM COMPUTES THE REAL PART OF THE COMPLEX
C  INTEGRAND F(Y) FOR A GIVEN Y USING THE SUBROUTINE ' DFUN '
C
      DOUBLE PRECISION FUNCTION TFR1(TY)
      IMPLICIT REAL*8(T)
      COMMON TUR,TKR,TKOA,TKOZ
      CALL DFUN(TUR,TKOZ,TKR,TKOA,TY,TRF,TIF)
      TFR1=TRF
      RETURN
      END
```

```
C  ***********************************************************************
C
C
C  THIS FUNCTION SUBPROGRAM COMPUTES THE IMAGINARY PART OF THE COMPLEX
C  INTEGRAND F(Y) FOR A GIVEN Y.
C
      DOUBLE PRECISION FUNCTION TFI(TY)
      IMPLICIT REAL*8(T)
      COMMON TUR,TKR,TKOA,TKOZ
      CALL DFUN(TUR,TKOZ,TKR,TKOA,TY,TRF,TIF)
      TFI=TIF
      RETURN
      END
```

```
C  ***********************************************************************
C
C
C  SUBROUTINE ' DFUN '.
C  THIS SUBROUTINE COMPUTES THE COMPLEX INTEGRAND F(Y) FOR A GIVEN Y.
C  THE COMPUTED RESULT OF THIS SUBROUTINE IS USED IN THE FUNCTION
C  SUBPROGRAMS 'TFR1 AND TFI ' TO OBTAIN THE REAL AND IMAGINARY PARTS
C  OF THE COMPLEX FUNCTION F(Y).
C
C
      SUBROUTINE DFUN(TUR,TKOZ,TKR,TKOA,TY,TRF,TIF)
      IMPLICIT COMPLEX*16(D),REAL*8(T)
      TYR=TY*TKOZ
      TPI=3.141592653D
      DX=TKOA*CDSQRT(1.D0-((1.D0+DCMPLX(0.D0,1.D0)*TY)**2))
      DZZ=TKOA*CDSQRT(TUR*TKR-((1.D0+DCMPLX(0.D0,1.D0)*TY)**2))
      DY=DX
      DU=DZZ
      YABS=CDABS(DX)
      IF (YABS.GE.20.D0) GO TO 5
      CALL BESH(DX,0,1,DH01V,IER)
      GO TO 10
    5 DX=DY
      CALL ASYZ(DX,0,1,DH01V)
   10 DX=DY
      YABS=CDABS(DX)
      IF (YABS.GE.20.D0) GO TO 15
      CALL BESH(DX,0,2,DH02V,IER)
      GO TO 20
   15 DX=DY
      CALL ASYS(DX,0,2,DH02V)
   20 DX=DY
      YABS=CDABS(DX)
      IF (YABS.GE.20.D0) GO TO 25
      CALL BESH(DX,1,2,DH12V,IER)
      GO TO 30
   25 DX=DY
      CALL ASYS(DX,1,2,DH12V)
   30 DX=DY
      YABS=CDABS(DX)
      IF (YABS.GE.20.D0) GO TO 35
      CALL BESH(DX,1,1,DH11V,IER)
      GO TO 40
   35 DX=DY
      CALL ASYS(DX,1,1,DH11V)
   40 YABS=CDABS(DZZ)
      IF (YABS.GE.20.D0) GO TO 45
      CALL BSIEHL(0,DZZ,DJ0U)
      GO TO 50
   45 CALL ASYA(DZZ,NORD,DJ0U)
   50 DZZ=DU
      YABS=CDABS(DZZ)
      IF (YABS.GE.20.D0) GO TO 55
      CALL BSIEHL(1,DZZ,DJ1U)
      GO TO 60
   55 DZZ=DU
      CALL ASYT(DZZ,1,DJ1U)
   60 DX=DY
      DZZ=DU
      DA=(DZZ*DJ0U*DH11V-TUR*DX*DJ1U*DH01V)
      DB=(DZZ*DJ0U*DH12V-TUR*DX*DJ1U*DH02V)
      DANS=(DJ1U**2)*TUR*(TUR-1.D3)*(TKOA**2)*DEXP(-TYR)/(DA*DB)
      TRF=REAL(DANS)
      TIF=AIMAG(DANS)
      RETURN
      END
```

```
C     ***********************************************************************
C
C
C     SUBROUTINE ' BESH '
C     THIS SUBROUTINE COMPUTES HANKEL FUNCTIONS OF COMPLEX ARGUMENTS.
C     FOR ABS.VALUE OF THE ARGUMENT < 50 AND 0 < PHASE < 180 DEGREES,
C     ATLEAST 5 FIGURE ACCURACY IS OBTAINED WHEN COMPARED WITH N.B.S.
C     TABLES. THIS SUBROUTINE DESTROYS ITS INPUT VALUES.
C
C
      SUBROUTINE BESH(DX,N,KIND,DWH,IER)
      IMPLICIT COMPLEX*16(D), REAL*8(T)
      DIMENSION DT(12)
      IF(N.EQ.0.AND.KIND.EQ.1) GO TO 300
      IF(N.EQ.0.AND.KIND.EQ.2) GO TO 400
      IF(N.EQ.1.AND.KIND.EQ.1) GO TO 300
      IF(N.EQ.1.AND.KIND.EQ.2) GO TO 400
  300 DX=DX*DCMPLX(0.D0,-1.D0)
      GO TO 500
  400 DX=DX*DCMPLX(0.D0,1.D0)
      GO TO 500
  500 TRX=REAL(DX)
      TIX=AIMAG(DX)
      TMAG=DSQRT(TRX**2+TIX**2)
      DEM=DCMPLX(0.D0,0.D0)
      TPI=3.14159265
      IF(N) 10,20,20
   10 IER=1
      RETURN
   20 IF (TMAG-170.D0) 22,22,21
   21 IER=5
      RETURN
   22 IER=0
      IF (TMAG-1.D0) 26,26,25
   25 DA=CDEXP(-DX)
      DB=1.D0/DX
      DC=CDSQRT(DB)
      IF(REAL(DC)) 100,101,101
  100 DC=-DC
  101 CONTINUE
      DT(1)=DB
      DO 26 L=2,12
   26 DT(L)=DT(L-1)*DB
      IF(N-1)27,29,27
C
C     COMPUTE K0 USING POLYNOMIAL APPROXIMATION
C
   27 DG0=DA*(1.25331410D0-.1306461800*DT(1)+.0981112780D0*DT(2)
     2+.0913990944D0*DT(3)+.1244036200*DT(4)-.2229050030*DT(5)
     3+.3792409760D0*DT(6)-.9243277300D0*DT(7)+.2973868400D0*DT(8)
     4-.4262632900D0*DT(9)+.2134518100*DT(10)-.0868(0760D0*DT(11)
     5-.0001893800D0*DT(12))*DC
      IF(N)30,28,30
   28 DBK=DG0
      GO TO 200
C
C     COMPUTE K1 USING POLYNOMIAL APPROXIMATION
C
   29 DG1=DA*(1.25331410D0+.4699927000*DT(1)-.1436838800*DT(2)
     2+.1280425600*DT(3)-.1736431400*DT(4)+.2847161800*DT(5)
     3-.4394162100*DT(6)+.6283380100*DT(7)-.6632299400*DT(8)
     4+.4903238600*DT(9)-.2381303800*DT(10)+.0788001200*DT(11)
     5-.0108434700D0*DT(12))*DC
      IF(N-1)120,30,31
   30 DBK=DG1
      GO TO 200
C
C     FROM K0,K1 COMPUTE KN USING RECURRENCE RELATION
C
   31 DO 33 J=2,N
      DGJ=2.D0*(FLOAT(J)-1.D0)*DG1/DBK*DG0
      IF(CDABS(DGJ)-1.D70) 32,32,32
   32 IER=4
      GO TO 34
   33 DG0=DG1
   35 DG1=DGJ
   34 DBK=DGJ
      GO TO 200
   36 DB=DX/2.D0
      IF (REAL(DB)) 70,71,70
   71 IF (AIMAG(DB)) 72,70,72
   72 YAMG=TPI/2.D0
      GO TO 75
   73 YAMG=TPI/2.D0
   75 YABS=CDABS(DB)
      YAR=0.5772156D0+DLOG(YABS)
      DA=DCMPLX(YAR,YAMG)
      GO TO 76
   70 DA=0.5772156D0+DLOG(DB)
   76 DC=DB*DA
      IF(N-1)40,41,27
C
C     COMPUTE K0 USING SERIES EXPANSION
C
   37 DGG=-DC
      DXJJ=DCMPLX(1.D0,0.D0)
      TFACT=1.D0
      TSUJ=0.D0
      DO 40 J=1,N
      TAJ=1.D0/FLOAT(J)
      DXJJ=DXJJ*DB
      TFACT=TFACT*TAJ*TAJ
      TSUJ=TSUJ+TAJ
   40 DGG=DGG+DXJJ*TFACT*(TSUJ-DAL
      IF(N)42,43,43
   41 DBK=DGG
```

```
0077          GO TO 240
C
C     COMPUTE K1 USING SERIES EXPANSION
C
0078       43 DKEJ=0D0
0079          TFACT=1.D0
0080          THJ=1.D0
0081          DK1=1.D0-DX*(DXJ*(1.D0D0/-THJ)
0082          DO 50 J=2,8
0083          DKEJ=DKEJ*DX
0084          TRJ=1.D0/FLOAT(J)
0085          TFACT=TFACT*TRJ*TRJ
0086          THJ=THJ*TRJ
0087       50 DK1=DK1+DKEJ*TFACT*(1.5D0+(DA-THJ)*FLOAT(J))
0088          IF(M-1)91,52,52
0089       52 DKM=DK1
C
C     COMPUTE HANKEL FUNCTION USING K0 AND K1
C
0090      200 IF(N.EQ.0.AND.M(KO.EQ.1) GO TO 110
0091          IF(N.EQ.0.AND.M(M1.EQ.2) GO TO 115
0092          IF(N.EQ.1.AND.M(KO.EQ.1) GO TO 120
0093          IF(N.EQ.1.AND.M(M1.EQ.2) GO TO 125
0094      110 DBM=-2.D0*DCMPLX(0.D0,1.D0)*DBK/TPI
0095          GO TO 130
0096      115 DBM=2.D0*DCMPLX(0.D0,1.D0)*DBK/TPI
0097          GO TO 130
0098      120 DBM=-2.D0*DBK/TPI
0099      125 CONTINUE
0100          RETURN
0101          END

C  ***********************************************************************
C
C
C  SUBROUTINE * BSLRML *
C  THIS SUBROUTINE COMPUTES BESSEL FUNCTION OF ORDER 0 AND 1 OF A
C  COMPLEX ARGUMENT.
C  FOR ABS.VALUE OF THE ARGUMENT <80 AND 0 < PHASE < 180 DEGREES
C  ATLEAST 5 FIGURE ACCURACY IS OBTAINED WHEN COMPARED WITH N.B.S.
C  TABLES. THIS SUBROUTINE DESTROYS ITS INPUT VALUES.
C
C
0001          SUBROUTINE  BSLRML(NORD,DZZ,DCBSLJ)
0002          IMPLICIT COMPLEX*16(A(D), REAL*8(T)
0003          N=NORD
0004          TX=REAL(DZZ)
0005          TY=AIMAG(DZZ)
0006          X=TX
0007          Y=TY
0008          TX=0.5D0*TX
0009          TY=0.5D0*TY
0010          TX=TX*TX-TY*TY
0011          TY=2.D0*TX*TY
0012          X=X
0013          BTC=10.0
0014          L=ISQRT(X*X+10.D0*(X*X+Y*Y))-X+BTC
0015          TPR=1.D0
0016          TPI=0.D0
0017          II=(L+1)*(X+L+1)
0018          JJ=-(X+L+X+1)
0019          DO 400 K=1,L
0020          TP=II+(JJ+K)*K
0021          TGR=TR/TP
0022          TGI=TB/TP
0023          TD=TPR
0024          TPR=1.D0-TGR*TPR+TGI*TPI
0025      400 TPI=-(TGR*TPI+TGI*TD)
0026          IF (N.EQ.0) GO TO 401
0027          IF (N.GT.0) GO TO 402
0028      401 CONTINUE
0029          DCBSLJ=DCMPLX(TPR,TPI)
0030          RETURN
0031      402 TGR=1.D0
0032          TGI=0.D0
0033          NN=N
0034      403 TC=TGI
0035          TGR=TGR*TX-TGI*TY
0036          TGI=TC*TY+TGI*TX
0037          NN=NN-1
0038          IF (NN.GT.0) GO TO 403
0039          TN=1.D0
0040          DO 404 NN=1,N
0041          NN=NN
0042      404 TN=TN*NN
0043          TGR=TGR/TN
0044          TGI=TGI/TN
0045          TD=TPR
0046          TPR=TPR*TGR-TPI*TGI
0047          TPI=TD*TGI+TPI*TGR
0048          GO TO 401
0049          END
```

```
C     ***********************************************************************
C
C
C     SUBROUTINES ' ASY2,ASY3,ASY4,ASY5,ASY6,ASY7 '.
C     THESE SUBROUTINES COMPUTE HANKEL AND BESSEL FUNCTIONS OF A COMPLEX
C     ARGUEMENT USING THE LARGE ARGUEMENT APPROXIMATIONS.
C
      SUBROUTINE ASY2(DX,N,KIND,DH01V)
      IMPLICIT COMPLEX*16(D), REAL*8(T)
      TPI=3.1415926500
      DH01V=CDSQRT(2.D0/(TPI*DX))
      DPHI=(DX-(TPI/4.D0))*DCMPLX(0.D0,1.D0)
      DH01V=DH01V*CDEXP(DPHI)
      RETURN
      END

C
      SUBROUTINE ASY3(DX,N,KIND,DH02V)
      IMPLICIT COMPLEX*16(D), REAL*8(T)
      TPI=3.1415926500
      DH02V=CDSQRT(2.D0/(TPI*DX))
      DPHI=-(DX-(TPI/4.D0))*DCMPLX(0.D0,1.D0)
      DH02V=DH02V*CDEXP(DPHI)
      RETURN
      END

C
      SUBROUTINE ASY4(DX,N,KIND,DH11V)
      IMPLICIT COMPLEX*16(D), REAL*8(T)
      TPI=3.1415926500
      DH11V=CDSQRT(2.D0/(TPI*DX))
      DPHI=(DX-(3.D0*TPI/4.D0))*DCMPLX(0.D0,1.D0)
      DH11V=DH11V*CDEXP(DPHI)
      RETURN
      END

C
      SUBROUTINE ASY5(DX,N,KIND,DH12V)
      IMPLICIT COMPLEX*16(D), REAL*8(T)
      TPI=3.1415926500
      DH12V=CDSQRT(2.D0/(TPI*DX))
      DPHI=-(DX-(3.D0*TPI/4.D0))*DCMPLX(0.D0,1.D0)
      DH12V=DH12V*CDEXP(DPHI)
      RETURN
      END

C
      SUBROUTINE ASY6(DZZ,NORD,DJ0U)
      IMPLICIT COMPLEX*16(D), REAL*8(T)
      TPI=3.1415926500
      DJ0U=CDSQRT(2.D0/(TPI*DZZ))
      DPHI=DZZ-(TPI/4.D0)
      DJ0U=DJ0U*CDCOS(DPHI)
      RETURN
      END

C
      SUBROUTINE ASY7(DZZ,NORD,DJ1U)
      IMPLICIT COMPLEX*16(D), REAL*8(T)
      TPI=3.1415926500
      DJ1U=CDSQRT(2.D0/(TPI*DZZ))
      DPHI=DZZ-(TPI*3.D0/4.D0)
      DJ1U=DJ1U*CDCOS(DPHI)
      RETURN
      END
```